Inorg. Chem. **2006**, *45*, 5661–5674

Inorganic Chemistry Article

Novel *tert*-Butyl-tris(3-hydrocarbylpyrazol-1-yl)borate Ligands: Synthesis, Spectroscopic Studies, and Coordination Chemistry[#]

Olivier Graziani,[†] Paul Hamon,[†] Jean-Yves Thépot,[†] Loïc Toupet,[‡] Petra Á. Szilágyi,[§] Gábor Molnár,[§] Azzedine Bousseksou,[§] Mats Tilset,*[,‖] and Jean-René Hamon*[,†]

UMR 6226 Sciences Chimiques de Rennes, CNRS–Université de Rennes 1, Campus de Beaulieu, 35042 Rennes Cedex, France, UMR 6626 Groupe Matière Condensée et Matériaux, CNRS–Université de Rennes 1, Campus de Beaulieu, 35042 Rennes Cedex, France, Laboratoire de Chimie de Coordination, LCC CNRS UPR 8241, Toulouse 205 route de Narbonne, 31077 Toulouse Cedex 4, France, and Department of Chemistry, University of Oslo, P. O. Box 1033 Blindern, N-0315 Oslo, Norway

Received March 17, 2006

The lithium (**1**) and thallium (**2**) salts of five new *tert*-butyl-tris(3-hydrocarbylpyrazol-1-yl)borate ligands [*t*-BuTp^{R}]$^-$ (R = H, **a**; Me, **b**; *i*-Pr, **c**; *t*-Bu, **d**; Ph, **e**) have been synthesized and characterized. Because of steric congestion at B, the reaction between *t*-BuBH$_3$Li•0.5Et$_2$O and excess 2,5-dimethylpyrazole Hpz^{Me2} afforded the bis-pz^{Me2} derivative, Tl[*t*-BuBH(3,5-Me$_2$pz)$_2$] (**3**) after metathesis with TlNO$_3$. The compounds were characterized by elemental analysis and NMR spectroscopy. The Li salts **1a** and **1c** exhibit fluxional behavior on the NMR time scale in solution at room temperature. The solid-state ^{7}Li and ^{11}B NMR spectra of **1c** suggest that this salt exists as a mixture of axial and equatorial isomers. The partial hydrolysis of **1d** afforded the dimeric Li complex {Li[*t*-BuB(pz^{t-Bu})$_2$(μ-OH)]}$_2$ (**4**). The crystal structure of **4** shows two Li cations encapsulated by the heteroscorpionate [*t*-BuB(OH)(3-*t*-Bupz)$_2$]$^-$ ligands. A salt elimination reaction between FeCl$_2$(THF)$_{1.5}$ and 2 equiv of Li[*t*-BuTp^{R}] (R = H, Me) followed by an in situ one-electron oxidation produced good yields of the homoleptic, paramagnetic low-spin iron(III) complexes [Fe(*t*-BuTp)$_2$]PF$_6$ (**5**) and [Fe(*t*-BuTp^{Me})$_2$]PF$_6$ (**6**) that were characterized by elemental analyses, magnetic susceptibility measurements in solution and the solid phase, ^{1}H NMR, high-resolution mass spectrometry, Mössbauer spectroscopy, and single-crystal X-ray diffraction. The crystals are composed of discrete molecular units with the central Fe(III) ion in an almost perfectly octahedral coordination to six nitrogen atoms. Compound **5** has the shortest Fe–N bond lengths ever reported for [Fe(RTp$^{R'}$)$_2$]$^+$-type compounds.

Introduction

The poly(1-pyrazol-1-yl)borates, nicknamed "scorpionates", were introduced by Trofimenko in the late 1960s[1] and are today well-established as ligands in coordination chemistry as evidenced by a large number of recent reviews.[2–9] The tris(pyrazolyl)borates usually act as facially coordinating six-electron ligands in a κ^3 coordination mode. Structural diversity arises when the substituents at B or at the 3, 4, and 5 positions of the pyrazolyl rings are altered. This permits the design of scorpionate ligands with very specific steric and electronic features. Among the simple [Tp^{R}]$^-$-type ligands with nonbulky R substituents at the 3 position,[10] the prototypical hydridotris(1-pyrazolyl)borate,[1,11] [Tp]$^-$, and its dimethylated analogue,[12] [Tp^{Me2}]$^-$, have been

* To whom correspondence should be addressed. Tel.: 33 2 23 23 59 58 (J.-R.H.). Fax: +33 2 23 23 56 37 (J.-R.H.), +47 22 85 54 41 (M.T.). E-mail: jean-rene.hamon@univ-rennes1.fr (J.-R.H.), mats.tilset@kjemi.uio.no (M.T.).

[#] This article is dedicated to Professor Didier Astruc, a distinguished friend and colleague, on the occasion of his 60th birthday.

[†] UMR 6226 Sciences Chimiques de Rennes, CNRS–Université de Rennes 1.

[‡] UMR 6626 Groupe Matière Condensée et Matériaux, CNRS–Université de Rennes 1.

[§] Laboratoire de Chimie de Coordination, LCC CNRS UPR 8241.

[‖] University of Oslo.

(1) Trofimenko, S. *J. Am. Chem. Soc.* **1966**, *88*, 1842–1844.
(2) Trofimenko, S. *Chem. Rev.* **1993**, *93*, 943–980.
(3) Trofimenko, S. *Scorpionates. The Chemistry of Polybyrazolylborate Ligands*; Imperial College Press: London, 1999.
(4) Trofimenko, S. *Polyhedron* **2004**, *23*, 197–203.
(5) Trofimenko, S. *J. Chem. Educ.* **2005**, *82*, 1715–1720.
(6) *Scorpionate and Related Ligands*; Parkin, G. F., Ed.; Polyhedron Symposia-In-Print Number 26, 2004; Vol. 23, pp 195–508.
(7) Pettinari, C.; Santini, C. *Comprehensive Coordination Chemistry II*; Elsevier: New York, 2004; Vol. 1, pp 159–210 and references cited.
(8) Marques, N.; Sella, A.; Takats, J. *Chem. Rev.* **2002**, *102*, 2137–2159.
(9) Edelmann, F. T. *Angew. Chem., Int. Ed.* **2001**, *40*, 1656–1660.

10.1021/ic060458n CCC: $33.50

Published on Web 06/17/2006

used extensively because of their availability. Poly(pyrazolyl)borates that bear relatively bulky alkyl or aryl substituents at the 3 position of the pyrazolyl rings introduced a new dimension in their coordination chemistry.[2−5] In particular, the use of the hydridotris(3-*tert*-butylpyrazolyl)borate, coined "tetrahedral enforcer", $[Tp^{t-Bu}]^-$,[13] and of its methyl[14] and phenyl[15] B-protected analogues, leads almost exclusively to the formation of four-coordinate compounds, although five- and six-coordinate Cr complexes of $[Tp^{t-Bu,Me}]^-$ have been structurally characterized.[16,17] The sterically less-hindered poly(3-phenyl)-, $[Tp^{Ph}]^-$,[13] and poly(3-isopropylpyrazolyl)borates, $[RTp^{i-Pr}]^-$ (R = H, pz^{i-Pr}),[18,19] permit the isolation of four- and five-coordinate complexes Tp^RMX_n ($n = 1, 2$). The $[Tp^{i-Pr}]^-$ ligand also forms octahedral M[HB(3-*i*-Prpz)$_2$(5-*i*-Prpz)]$_2$ compounds in which one 3-*i*-Prpz ring has rearranged to the 5-substituted isomer.[18,19] Interestingly, the high-spin six-coordinate iron(II) complex $Fe[Tp^{Ph}]_2$ has all six phenyl groups in the equatorial belt.[20] To prevent the 3,3,3/3,3,5 ligand rearrangement, or to make it degenerated, and at the same time to keep the advantageous characteristics (shielding effect, solubility, and electron donor properties) of a 3-isopropyl substituent, Kitajima et al.[21] introduced the hydridotris(3,5-diisopropyl-1-pyrazolyl)borate ligand, $[Tp^{i-Pr2}]^-$. The fascinating organometallic and inorganic chemistry of this ligand system has since been developed by Akita, Hikichi, and Moro-oka.[22−24]

Recently, species in which the hydride at boron is replaced by other groups have attracted attention. Interestingly, a substitution at boron by a simple alkyl or aryl group[14,15,25−27] can induce dramatic changes in the electronic and steric characteristics of $M[RTp^X]$ complexes. For example, the octahedral iron(II) compounds $Fe[PhTp]_2$ and $Fe[pzTp]_2$ are diamagnetic,[28] whereas the unsubstituted analogue $Fe[Tp]_2$ exhibits a spin equilibrium in solution at room temperature.[29] The thallium salts of phenyl-tris(3-*tert*-butylpyrazolyl)borate $[PhTp^{t-Bu}]^-$,[15] methyl-tris(3,5-dimethylpyrazol-1-yl)borate $[MeTp^{Me2}]^-$,[27] and the organometallics-substituted scorpionate ligands $[RTp^{R'}]^-$ [R = (η^5-C_5H_5)Fe(η^5-C_5H_4)[30−33] and (η^5-C_5H_3Me)$Mn(CO)_3$[34]] do not conform to the classical tridentate, C_3-symmetrical coordination mode at thallium. Rather, as a consequence of steric crowding at the boron in these four complexes, one pyrazolyl group is rotated by ca. 90° around the B−N axis, resulting in unprecedented monomeric,[15] polymeric,[30−34] and helicoidal chain[27] structures. The replacement of the hydride at boron with neutral or anionic functional groups X provides a possible reactive center or coordination site on the "outside" of the TpM moiety. For example, ligands of the type $[p\text{-}XC_6H_4Tp^R]^-$ that are specifically functionalized at the noncoordinating "outside" position were first reported by Faller and White[35] and more recently by Reger and co-workers,[36,37] who showed the profound impact of the resulting supramolecular structures on the electronic spin-state crossover properties of the corresponding iron(II) complexes.[36]

We were interested in exploring how the introduction of a boron *tert*-butyl substituent in conjunction with various 3 substituents would affect the coordinating behavior of the resulting homoscorpionate ligands. The innocent *tert*-butyl spectator substituent at boron was chosen to prevent possible ligand degradation via reactions at the B−H bond, to increase ligand solubility in less-polar solvents, to suppress the 3/5 isomerization of a 3-substituted pyrazolyl ring, and to use it as an NMR probe. We now report on (i) the syntheses and structures of a new family of *tert*-butyl substituted tris(3-hydrocarbylpyrazol-1-yl)borate complexes, $M[t\text{-}BuTp^R]$ (M = Li, Tl; R = H, Me, *i*-Pr, *t*-Bu, Ph), (ii) the hydrolytic cleavage of one B−N bond of $Li[t\text{-}BuTp^{t-Bu}]$ leading to the isolation and X-ray characterization of the dimeric heteroscorpionate $\{Li[t\text{-}BuB(pz^{t-Bu})_2(\mu\text{-}OH)]\}_2$, and (iii) some aspects of the coordination chemistry of these ligands toward Fe. We recently communicated[38] the reaction between $FeCl_2(THF)_{1.5}$ and $Tl[t\text{-}BuTp^{t-Bu}]$, which proceeds by an unexpected deboronation reaction with the cleavage of the three

(10) The abbreviations adopted here for hydridotris(pyrazolyl)borato ligands are based on those proposed by Trofimenko in ref 2. Thus, the hydridotris(pyrazolyl)borato ligands are represented by the abbreviation $[Tp]^-$, with the 3- and 5-alkyl or aryl substituents listed respectively as superscripts, $[Tp^{R,R'}]^-$. If the fourth substituent on boron is anything other than hydrogen, the substituent is listed as a prefix, e.g., $[RTp]^-$ and $[t\text{-}BuTpR]^-$. The same abbreviation system stands for the pyrazolyl ring, e.g., pz and pz^R.

(11) Trofimenko, S. *J. Am. Chem. Soc.* **1967**, *89*, 3170−3177.
(12) Trofimenko, S. *J. Am. Chem. Soc.* **1967**, *89*, 6288−6294.
(13) Trofimenko, S.; Calabrese, J. C.; Thompson, J. S. *Inorg. Chem.* **1987**, *26*, 1507−1514.
(14) Dias, H. V. R.; Wang, X. *Polyhedron* **2004**, *23*, 2533−2539.
(15) Kisko, J. L.; Hascall, T.; Kimblin, C.; Parkin, G. *J. Chem. Soc., Dalton Trans.* **1999**, 1929−1936.
(16) Hess, A.; Hörz, M. R.; Liable-Sands, L. M.; Lindner, D. C.; Rheingold, A. L.; Theopold, K. H. *Angew. Chem., Int. Ed.* **1999**, *38*, 166−168.
(17) Qin, K.; Incarvito, C. D.; Rheingold, A. L.; Theopold, K. H. *Angew. Chem., Int. Ed.* **2002**, *41*, 2333−2335.
(18) Trofimenko, S.; Calabrese, J. C.; Domaille, P. J.; Thompson, J. S. *Inorg. Chem.* **1989**, *28*, 1091−1101.
(19) Calabrese, J. C.; Domaille, P. J.; Thompson, J. S.; Trofimenko, S. *Inorg. Chem.* **1990**, *29*, 4429−4437.
(20) Eichhorn, D. M.; Armstrong, W. H. *Inorg. Chem.* **1990**, *29*, 3607−3612.
(21) Kitajima, N.; Fujisawa, K.; Fujimoto, C.; Moro-oka, Y.; Hashimoto, S.; Kitagawa, T.; Toriumi, K.; Tatsumi, K.; Nakamura, A. *J. Am. Chem. Soc.* **1992**, *114*, 1277−1291.
(22) Akita, M. *J. Organomet. Chem.* **2004**, *689*, 4540−4551.
(23) Akita, M.; Hikichi, S. *Bull. Chem. Soc. Jpn.* **2002**, *75*, 1657−1679.
(24) Moro-oka, Y. *Proc. Ind. Acad. Sci., Chem. Sci.* **1999**, *111*, 413−424.
(25) Kisko, J. L.; Hascall, T.; Parkin, G. *J. Am. Chem. Soc.* **1998**, *120*, 10561−10562.
(26) Dias, H. V. R.; Wang, X.; Diyabalanage, H. V. K. *Inorg. Chem.* **2005**, *44*, 7322−7324.
(27) Janiak, C.; Braun, L.; Girgsdies, F. *J. Chem. Soc., Dalton Trans.* **1999**, 3133−3136.
(28) Sohrin, Y.; Kokusen, H.; Matsui, M. *Inorg. Chem.* **1995**, *34*, 3928−3934.
(29) Jesson, J. P.; Trofimenko, S.; Eaton, D. R. *J. Am. Chem. Soc.* **1967**, *89*, 3158−3164.
(30) Jäkle, F.; Polborn, K.; Wagner, M. *Chem. Ber.* **1996**, *129*, 603−606.
(31) Fabrizi de Biani, F.; Jäkle, F.; Spiegler, M.; Wagner, M.; Zanello, P. *Inorg. Chem.* **1997**, *36*, 2103-2111.
(32) Herdtweck, E.; Peters, F.; Scherer, W.; Wagner, M. *Polyhedron* **1998**, *17*, 1149−1157.
(33) Guo, S.; Peters, F.; Fabrizi de Biani, F.; Bats, J. W.; Herdtweck, E.; Zanello, P.; Wagner, M. *Inorg. Chem.* **2001**, *40*, 4928−4936.
(34) Guo, S.; Bats, J. W.; Bolte, M.; Wagner, M. *J. Chem. Soc., Dalton Trans.* **2001**, 3572−3576.
(35) White, D. L.; Faller, J. W. *J. Am. Chem. Soc.* **1982**, *104*, 1548−1552.
(36) Reger, D. L.; Gardinier, J. R.; Gemmill, W. R.; Smith, M. D.; Shahin, A. M.; Long, G. J.; Rebbouh, L.; Grandjean, F. *J. Am. Chem. Soc.* **2005**, *127*, 2303−2316.
(37) Reger, D. L.; Gardinier, J. R.; Smith, M. D.; Shahin, A. M.; Long, G. J.; Rebbouh, L.; Grandjean, F. *Inorg. Chem.* **2005**, *44*, 1852−1866.
(38) Graziani, O.; Toupet, L.; Hamon, J.-R.; Tilset, M. *Inorg. Chim. Acta* **2002**, *341*, 127−131.

boron−nitrogen bonds to form the structurally characterized high-spin d^6 Fe(II) complex *trans*-$FeCl_2(Hpz^{t-Bu})_4$.

Experimental Section

CAUTION! *Thallium and its compounds are toxic and should be handled with caution using appropriate safety procedures. Contact with the skin and inhalation of the dust should be avoided; wastes should be collected and disposed of separately as heavy metal waste. Care must be taken in destroying residual alanes (from the purification of $LiAlH_4$ and the preparation of t-BuH_3Li). This destruction must be carried out at low temperatures (−78 °C) under argon by the slow addition of ethyl acetate.*

General Procedures. All reactions were carried out under an argon atmosphere using Schlenk techniques or in a Jacomex 532 drybox filled with argon. The isolated complexes were relatively stable in the air, where they can be weighed, but were nevertheless stored under an inert atmosphere at room temperature. Infrared spectra were obtained as Nujol mulls or as KBr pellets with a Bruker IFS28 FTIR infrared spectrophotometer (400−4000 cm^{-1}). ^{1}H and ^{13}C NMR spectra were recorded on a multinuclear Bruker DPX 200 spectrometer (200 MHz) at 297 K, and all chemical shifts are reported in ppm (δ) relative to tetramethylsilane, using the residual solvent resonances as internal references. ^{11}B NMR spectra were reported relative to external $BF_3{\cdot}Et_2O$. Variable-temperature ^{1}H and ^{7}Li NMR spectra were acquired with a Bruker AM300WB spectrometer (300 MHz for ^{1}H). The temperature of the NMR probe was controlled by a Bruker VT unit, and the temperature calibration was accomplished with Van Geet's methanol method[39] and found to be accurate to within 1 °C. ^{13}C cross polarization magic angle spinning (CPMAS) NMR spectra (125.77 MHz) were recorded on a Bruker AVANCE500 instrument at 300 K using a 4 mm probe head and rotational frequencies of 10 and 14 kHz. ^{7}Li MAS (116.6 MHz) and ^{11}B MAS (96.25 MHz) NMR spectra were obtained on a Bruker ASX300 spectrometer using a 4 mm probe head and rotation frequencies of 6 and 9 kHz for ^{7}Li and 14 and 15 kHz for ^{11}B. Samples were carefully packed in ZrO_2 rotors, and the standard CPMAS and MAS sequences were employed. Chemical shifts in ppm (δ) are referred to Me_4Si, LiCl, and $BF_3{\cdot}Et_2O$. Melting points were measured with a Kofler device. Mass spectrometric measurements were performed at the Centre Régional de Mesures Physiques de l'Ouest (CRMPO) Rennes, on a high-resolution ZabSpec TOF VG Analytical spectrometer operating in the ESI$^+$ mode; poly(ethylene glycol) was used as an internal reference, and dichloromethane was used as a solvent. All mass measurements refer to peaks for the most common isotopes (^{1}H, ^{11}B, ^{12}C, ^{14}N, and ^{56}Fe). Solution magnetic susceptibility measurements were done with Evans' method.[40−42] Mössbauer spectra were recorded using a constant-acceleration-type spectrometer equipped with a ^{57}Co source (15 mCi). Spectra were recorded at 80 and 293 K in a flow-type liquid-nitrogen cryostat. Least-squares fittings of the Mössbauer spectra were carried out with the assumption of Lorentzian line shapes using the MossWinn 3.0 program.[43] Mössbauer isomer shifts are given relative to natural iron at room temperature. Elemental analyses were carried out at the Service Central d'Analyse, USR CNRS 56, Vernaison, France, and by Ilse Beetz Microanalytisches Laboratorium, Kronach, Germany.

Materials. Reagent grade tetrahydrofuran, toluene, pentane, and diethyl ether were predried and distilled under argon from blue-purple solutions of sodium benzophenone ketyl prior to use. Dichloromethane was distilled under argon from P_2O_5. All glassware was oven-dried and vacuum or argon flow degassed before use. Reagents were obtained as follows: Pyrazole, 3,5-dimethylpyrazole (Aldrich), 3(5)-methylpyrazole, $TlNO_3$, and 1,3-propanediol (Acros) were used as received. Trimethoxyborane (Acros) was distilled under argon before use. Commercial $LiAlH_4$ (Aldrich) was purified by dissolution in Et_2O (1 g/10 mL; sequential addition of small quantities) at room temperature. After stirring for 1.5 h, the solution was filtered off and evaporated to dryness. The white powder was then washed twice with pentane and dried in vacuo. The so purified $LiAlH_4$ was kept under argon. Lithium *tert*-butylborohydride ether solvate (*t*-$BuBH_3Li.0.5Et_2O$),[44] 3(5)-*tert*-butylpyrazole,[13] 3(5)-phenylpyrazole,[13] 3(5)-isopropylpyrazole,[18] and $FeCl_2(THF)_{1.5}$ [which assumes the tetranuclear $Fe_4Cl_8(THF)_6$ form in the solid state][45,46] were prepared according to literature procedures.

Lithium *tert*-Butyl[tris(3-R-pyrazolyl)]borate, Li[*t*-BuTp^R] (1a−e). General Procedure. A three-necked 500 mL round-bottom flask fitted with a water-cooled condenser was charged with a magnetic stir bar, *t*-$BuBH_3Li{\cdot}0.5Et_2O$, and a slight excess (ca. 3.4 equiv) of the desired pyrazole (3-RpzH). The mixture was stirred and heated, first at 120 °C until the evolution of hydrogen ceased. The stirring was continued while the temperature was increased to 220 °C. The reaction mixture was kept at this temperature until the further evolution of hydrogen stopped and was cooled to room temperature affording a solid white block. The solid material was carefully broken into small pieces with a spatula and poured into a beaker where it was finely ground. The white powder was stirred in 100 mL of hexane, filtered, and dried in vacuo. This crude material could be used to make *t*-BuTp^R complexes without further purification.

(a) R = H: Li[*t*-BuTp] (1a). *t*-$BuBH_3Li{\cdot}0.5Et_2O$, 2.50 g (22.0 mmol); pyrazole, 5.90 g (73.0 mmol); 1 h at 120 °C and 12 h at 220 °C. Yield: 5.66 g (19.8 mmol, 90%). ^{1}H NMR (CD_3COCD_3): δ 7.55 (br s, 3 H, H-5), 6.92 (d, 3 H, H-3, $^3J_{H-H}$ = 2.0 Hz), 6.14 (dd, 3 H, H-4, $^3J_{H-H}$ = 2.0 Hz, $^3J_{H-H}$ = 1.8 Hz), 0.84 (s, 9 H, *t*-Bu).

(b) R = Me: Li[*t*-BuTp^{Me}] (1b). *t*-$BuBH_3Li{\cdot}0.5Et_2O$, 3.27 g (28.4 mmol); 3(5)-methylpyrazole, 9.2 mL (114 mmol); 2 h at 120 °C, 1 h at 180 °C, and 12 h at 220 °C. The excess of methylpyrazole was removed under a vacuum at 170 °C (8 mm Hg), and the white residue was ground, stirred into 100 mL of pentane, filtered, and dried in vacuo. Yield: 8.0 g (25.2 mmol, 89%). ^{1}H NMR (CD_3COCD_3): δ 6.78 (d, 3 H, H-5, $^3J_{H-H}$ = 2.2 Hz), 5.88 (d, 3 H, H-4, $^3J_{H-H}$ = 2.2 Hz), 2.26 (s, 9 H, CH_3), 0.78 (s, 9 H, *t*-Bu). ^{13}C{^{1}H} NMR (CD_3COCD_3): δ 147.4 (C-3), 136.0 (C-5), 102.9 (C-4), 28.9 [$BC(CH_3)_3$], 13.5 (CH_3).

(c) R = *i*-Pr: Li[*t*-BuTp^{i-Pr}] (1c). *t*-$BuBH_3Li{\cdot}0.5Et_2O$, 5.71 g (50.0 mmol); 3(5)-isopropylpyrazole, 19.1 g (174.0 mmol); 1 h at 120 °C and 5 h at 220 °C. The excess of isopropylpyrazole was distilled under a vacuum at 170 °C (8 mm Hg), and the white residue was ground, stirred into 100 mL of hexane, filtered, and dried in vacuo. Yield: 42.0 g (36.0 mmol, 72%). ^{1}H NMR

(39) Van Geet, A. L. *Anal. Chem.* **1970**, *42*, 679−680.
(40) Evans, D. F. *J. Chem. Soc.* **1959**, 2003−2005.
(41) Crawford, T. H.; Swanson, J. *J. Chem. Educ.* **1971**, *48*, 382−386.
(42) Schubert, E. M. *J. Chem. Educ.* **1992**, *69*, 62.
(43) Klencsár, Z.; Kuzmann, E.; Vértes, A. *J. Radioanal. Nucl. Chem.* **1996**, *210*, 105−118.
(44) Srebnik, M.; Cole, T. E.; Ramachandran, P. V.; Brown, H. C. *J. Org. Chem.* **1989**, *54*, 6085−6096.
(45) Bel'skii, V. K.; Ishchenko, V. M.; Bulychev, B. M.; Protskii, A. N.; Soloveichik, G. L.; Ellert, O. G.; Seifulina, Z. M.; Rakitin, Y.; Novotortsev, V. M. *Inorg. Chim. Acta* **1985**, *96*, 123−127.
(46) Cotton, F. A.; Luck, R. L.; Son, K. A. *Inorg. Chim. Acta* **1991**, *179*, 11−15.

(CD_3COCD_3): δ 6.81 (d, 3 H, H-5, $^3J_{H-H}$ = 2.2 Hz), 5.96 (d, 3 H, H-4, $^3J_{H-H}$ = 2.2 Hz), 3.08 (sept, 3 H, C*H*(CH_3)$_2$, $^3J_{H-H}$ = 7.0 Hz), 1.25 (d, 18 H, CH(C*H*$_3$)$_2$, $^3J_{H-H}$ = 7.0 Hz), 0.79 (s, 9 H, *t*-Bu). ^{11}B NMR (CD_3COCD_3, 96.28 MHz): δ 3.79 (br s).

(d) R = *t*-Bu: Li[*t*-BuTp^{t-Bu}] (1d). *t*-BuBH$_3$Li·0.5Et$_2$O, 2.53 g (22.0 mmol); 3(5)-*tert*-butylpyrazole, 9.0 g (73.0 mmol); 1 h at 120 °C and 5 h at 220 °C. Purification was performed as described above for Li[*t*-BuTp^{i-Pr}] with vacuum distillation of the excess *tert*-butylpyrazole at 190 °C (8 mm Hg). Yield: 8.0 g (18.0 mmol, 82%). ^{1}H NMR (CD_3COCD_3): δ 6.80 (d, 3 H, H-5, $^3J_{H-H}$ = 2.2 Hz), 5.98 (d, 3 H, H-4, $^3J_{H-H}$ = 2.2 Hz), 1.33 (s, 27 H, *t*-Bu-pz), 0.88 (s, 9 H, *t*-Bu-B).

(e) R = Ph: Li[*t*-BuTp^{Ph}] (1e). *t*-BuBH$_3$Li·0.5Et$_2$O, 3.53 g (30.1 mmol); 3(5)-phenylpyrazole, 14.61 g (101.0 mmol); 1 h at 120 °C and 12 h at 220 °C. Yield: 9.95 g (19.2 mmol, 64%). ^{1}H NMR (CD_3COCD_3): δ 7.91−7.86 (m, 6 H, Ph), 7.42−7.23 (m, 9 H, Ph), 7.08 (d, 3 H, H-5, $^3J_{H-H}$ = 2.4 Hz), 6.54 (d, 3 H, H-4, $^3J_{H-H}$ = 2.4 Hz), 1.09 (s, 9 H, *t*-Bu).

Thallium *tert*-Butyl[tris(3-R-pyrazolyl)]borate, Tl[*t*-BuTp^R] (2a−e). General Procedure. The solid lithium salts Li[*t*-BuTp^R] (**1a**−**e**), prepared as described above, were dissolved in methanol. The addition of an aqueous thallium nitrate (1.1 equiv) solution caused the immediate precipitation of a white powder. The solid was filtered, thoroughly washed twice with methanol (50 mL), and dried in vacuo. For the five compounds **2a**−**e**, the tertiary C atom [B-*C*(CH_3)$_3$] bonded to the boron atom was never observed in the ^{13}C NMR spectra.

(a) R = H: Tl[*t*-BuTp] (2a). Li[*t*-BuTp] (**1a**), 1.00 g (3.62 mmol) in 30 mL of methanol; TlNO$_3$, 1.10 g (4.0 mmol) in 15 mL of water. Yield: 1.31 g (2.31 mmol, 65%). mp: 238−240 °C. Anal. Calcd for $C_{13}H_{18}BN_6Tl$: C, 32.98; H, 3.83; N, 17.75. Found: C, 33.10; H, 3.83; N, 17.32. ^{1}H NMR (CD_3COCD_3): δ 7.60 (d, 3 H, H-5, $^3J_{H-H}$ = 1.8 Hz), 7.17 (d, 3 H, H-3, $^3J_{H-H}$ = 2.0 Hz), 6.24 (dd, 3 H, H-4, $^3J_{H-H}$ = 2.0 Hz, $^3J_{H-H}$ = 1.8 Hz), 0.92 (s, 9 H, *t*-Bu). ^{13}C{^{1}H} NMR (CD_3COCD_3): δ 139.2 (C-3), 136.5 (C-5), 104.5 (C-4), 29.5 [BC(C*H*$_3$)$_3$].

(b) R = Me: Tl[*t*-BuTp^{Me}] (2b). Li[*t*-BuTp^{Me}] (**1b**), 0.5 g (1.57 mmol) in 10 mL of methanol; TlNO$_3$, 0.43 g (1.60 mmol) in 50 mL of water. Because **2b** is slightly soluble in methanol, the white precipitate was washed with water (2 × 30 mL), dissolved in 30 mL of CH_2Cl_2, and dried over MgSO$_4$. After filtration, the solvent was evaporated and the white residue washed with 5 mL of cold pentane (−20 °C) and dried in vacuo. Yield: 0.73 g (1.42 mmol, 90%); no mp detected up to 265 °C. Anal. Calcd for $C_{16}H_{24}BN_6Tl$: C, 37.27; H, 4.70; N, 16.30. Found: C, 37.67; H, 4.31; N, 16.37. ^{1}H NMR (CD_3COCD_3): δ 7.55 (d, 3 H, H-5, $^3J_{H-H}$ = 2.2 Hz), 6.12 (d, 3 H, H-4, $^3J_{H-H}$ = 2.2 Hz), 2.33 (s, 9 H, Me), 0.87 (s, 9 H, *t*-Bu). ^{13}C{^{1}H} NMR (CD_3COCD_3): δ 143.2 (C-3), 134.5 (C-5), 104.5 (C-4), 27.0 [C(C*H*$_3$)$_3$], 11.3 (Me).

(c) R = *i*-Pr: Tl[*t*-BuTp^{i-Pr}] (2c). Li[*t*-BuTp^{i-Pr}] (**1c**), 1.43 g (3.55 mmol) in 10 mL of methanol; TlNO$_3$, 1.05 g (3.9 mmol) in 50 mL of water. Yield: 1.46 g (2.4 mmol, 69%). mp: 120−122 °C. Anal. Calcd for $C_{22}H_{36}BN_6Tl$: C, 44.06; H, 6.05; N, 14.01. Found: C, 43.87; H, 5.97; N, 14.04. ^{1}H NMR (CD_3COCD_3): δ 7.35 (d, 3 H, H-5, $^3J_{H-H}$ = 2.0 Hz), 6.12 (d, 3 H, H-4, $^3J_{H-H}$ = 2.2 Hz), 3.13 (sept, 3 H, C*H*(CH_3)$_2$, $^3J_{H-H}$ = 6.8 Hz), 1.27 (d, 18 H, CH(C*H*$_3$)$_2$, $^3J_{H-H}$ = 6.8 Hz), 1.02 (s, 9 H, *t*-Bu). ^{13}C{^{1}H} NMR (CD_3COCD_3): δ 159.5 (C-3), 136.3 (C-5), 100.9 (C-4), 30.0 [C(C*H*$_3$)$_3$], 27.9 [*C*H(CH_3)$_2$], 23.6 [CH(*C*H$_3$)$_2$].

(d) R = *t*-Bu: Tl[*t*-BuTp^{t-Bu}] (2d). Li[*t*-BuTp^{t-Bu}] (**1d**), 1.03 g (2.32 mmol) in 5 mL of methanol; TlNO$_3$, 0.68 g (2.55 mmol) in 25 mL of water. Yield: 0.79 g (1.6 mmol, 70%). mp: 212−214 °C. Anal. Calcd for $C_{25}H_{42}BN_6Tl$: C, 46.78; H, 6.60; N, 13.09. Found: C, 46.66; H, 6.60; N, 12.87. ^{1}H NMR (CD_3COCD_3): δ 7.66 (d, 3 H, H-5, $^3J_{H-H}$ = 2.4 Hz), 6.20 (d, 3 H, H-4, $^3J_{H-H}$ = 2.2 Hz), 1.32 (s, 27 H, *t*-Bu-pz), 1.10 (s, 9 H, *t*-Bu-B). ^{13}C{^{1}H} NMR (CD_3COCD_3): δ 162.7 (C-3), 136.0 (C-5), 101.7 (C-4), 32.2 [(CH_3)$_3$*C*-pz], 31.4 [(*C*H$_3$)$_3$C-pz], 30.7 [(*C*H$_3$)$_3$C−B].

(e) R = Ph: Tl[*t*-BuTp^{Ph}] (2e). Li[*t*-BuTp^{Ph}] (**1e**), 1.00 g (1.98 mmol) in 15 mL of methanol; TlNO$_3$, 0.58 g (2.2 mmol) in 15 mL of water. Yield: 1.00 g (1.4 mmol, 72%). mp: 178−180 °C. Anal. Calcd for $C_{31}H_{30}BN_6Tl$: C, 53.06; H, 4.31; N, 11.97. Found: C, 53.12; H, 4.48; N, 11.95. ^{1}H NMR (CD_3COCD_3): δ 7.87−7.82 (m, 6 H, Ph), 7.45−7.30 (m, 9 H, Ph), 7.41 (d, 3 H, H-5, $^3J_{H-H}$ = 2.2 Hz), 6.68 (d, 3 H, H-4, $^3J_{H-H}$ = 2.4 Hz), 1.15 (s, 9 H, *t*-Bu). ^{13}C{^{1}H} NMR (CD_3COCD_3): δ 152.2 (C-3), 137.5 (C-5), 134.9 (C$_{ipso}$ Ph), 129.1 (*o*-C Ph), 127.6 (*p*-C Ph), 126.4 (*m*-C Ph), 102.7 (C-4), 29.6 (C(*C*H$_3$)$_3$).

Thallium *tert*-Butyl[bis(3,5-dimethylpyrazolyl)]borate, Tl[*t*-BuBH(pz^{Me2})$_2$] (3). A three-necked 500 mL round-bottom flask fitted with a water-cooled condenser was charged with a magnetic stir bar, *t*-BuBH$_3$Li·0.5Et$_2$O (2.40 g, 21.0 mmol), and 3,5-dimethylpyrazole (8.0 g, 84.0 mmol). The mixture was stirred and heated first at 120 °C until the evolution of hydrogen ceased (1 h). The melt was then heated to 220 °C for 16 h. The mixture was cooled to room temperature, affording a solid block. Extraction as described above for Li[*t*-BuTp^R] salts provided a white powder which was washed with 50 mL of pentane, filtered, and dried in vacuo. This crude off-white solid was then dissolved in 50 mL of methanol, and an aqueous solution of TlNO$_3$ (6.0 g, 21.0 mmol) was added. A white precipitate formed immediately. It was collected on a glass frit, thoroughly washed with 2 × 30 mL of methanol, and dried in vacuo. Yield: 2.0 g (7.0 mmol, 33%). mp: 164−166 °C. Anal. Calcd for $C_{14}H_{24}BN_4Tl$: C, 36.28; H, 5.22; N, 12.09. Found: C, 36.32; H, 5.31; N, 12.12. IR (Nujol, cm^{-1}): ν_{BH} 2458. ^{1}H NMR (CD_3COCD_3): δ 5.77 (s, 2 H, H-4), 2.35, 2.34 (two s, each 6 H, Me), 0.76 (s, 9 H, *t*-Bu). ^{13}C{^{1}H} NMR (CD_3COCD_3): δ 146.4 (C-3 or C-5), 145.5 (C-5 or C-3), 105.2 (C-4), 29.8 [C(*C*H$_3$)$_3$], 13.6, 12.5 (Me).

{Li[*t*-BuB(pz^{t-Bu})$_2$(μ-OH)]}$_2$ (4). This reaction was performed without any precautions to exclude air, moisture, and light. In a well-ventilated fume hood, Li[*t*-BuTp^{t-Bu}] (**1d**; 0.500 g, 1.125 mmol) was dissolved in 5 mL of benzene in an open beaker and heated to 50 °C until it was completely dissolved. The solution was filtered through a filter funnel filled with glass wool into an Erlenmeyer flask and allowed to slowly cool in the fume hood. After 5 days, well-shaped colorless crystals deposited. They were collected by filtration on a glass frit and dried under a nitrogen stream. Yield: 0.364 g (0.40 mmol, 70%). Some crystals were subjected to elemental analysis, whereas an especially well-shaped one was selected for X-ray diffraction study. Anal. Calcd for $C_{50}H_{88}B_2Li_2N_{12}O_2$: C, 64.94; H, 9.59; N, 18.17. Found: C, 64.71; H, 9.60; N, 18.18. The rest of the crystals were ground in a mortar and dried at 170 °C (8 mm Hg) for 16 h in order to remove the free *tert*-butylpyrazole. ^{1}H NMR (CDCl$_3$): δ 7.53 (d, 4 H, H-5, $^3J_{H-H}$ = 2.0 Hz), 6.18 (d, 4 H, H-4, $^3J_{H-H}$ = 2.0 Hz), 1.40 (s, 18 H, *t*-Bu-B), 1.32 (s, 36 H, *t*-Bu-pz).

Bis{*tert*-butyl[tris(pyrazolyl)]borato}iron(III) Hexafluorophosphate, [Fe(*t*-BuTp)$_2$]PF$_6$ (5). To a pale green solution of FeCl$_2$(THF)$_{1.5}$ (0.166 g, 0.71 mmol) in dichloromethane (30 mL) was added solid Li[*t*-BuTp] (**1a**; 0.429 g, 1.55 mmol). A pink slurry formed immediately upon stirring that was maintained for 6 h. Then, ferrocenium hexafluorophosphate (0.222 g, 0.67 mmol) and 30 mL of dichloromethane were added to the reaction mixture, and the stirring was continued for 16 h. The dark blue suspension progressively turned red. After filtration to leave LiCl behind and

Table 1. Crystal, Data Collection, and Structure Refinement Parameters for compounds **4**−**6**

	4	**5**	**6**
empirical formula	$C_{50}H_{88}B_2Li_2N_{12}O_2$	$C_{26}H_{36}B_2F_6FeN_{12}P{\cdot}CH_2Cl_2$	$C_{32}H_{48}B_2F_6FeN_{12}P$
formula mass, g mol^{-1}	924.82	824.03	823.26
collection *T*, K	150(2)	110 (2)	293(2)
cryst syst	triclinic	monoclinic	orthorhombic
space group	$P\bar{1}$	$P2_1/n$	*Pbcn*
a (Å)	11.2991(3)	11.6712(2)	10.0554(1)
b (Å)	11.5788(3)	21.5213(3)	18.6230(3)
c (Å)	11.6144(4)	14.5322(2)	20.5137(3)
α (deg)	86.3070(10)	90.0	90.0
β (deg)	85.5870(10)	100.3087(5)	90.0
γ (deg)	70.603(2)	90.0	90.0
V (Å^3)	1427.80(7)	3591.27(9)	3841.43(9)
Z	2	4	4
D_{calcd} (g cm^{-3})	1.076	1.524	1.423
cryst size (mm)	0.36 × 0.21 × 0.14	0.25 × 0.12 × 0.12	0.28 × 0.24 × 0.24
F(000)	504	1692	1716
abs coeff (mm^{-1})	0.660	0.685	0.506
θ range (deg)	1.76−27.47	2.27−27.49	2.30−27.50
range *h,k,l*	0/14, −13/15, −14/15	0/15, 0/27, −18/18	0/13, 0/24, 0/26
unique reflns	6414	8213	4402
reflns [$I > 2\sigma(I)$]	4374	5615	3263
data/restraints/parameters	6414/0/311	8213/0/464	4402/0/248
final *R* indices [$I > 2\sigma(I)$]	$R_1 = 0.0499$ $wR_2 = 0.1251$	$R_1 = 0.0508$ $wR_2 = 0.1235$	$R_1 = 0.0549$ $wR_2 = 0.1629$
R indices (all data)	$R_1 = 0.0848$ $wR_2 = 0.1466$	$R_1 = 0.0886$ $wR_2 = 0.1434$	$R_1 = 0.0751$ $wR_2 = 0.1828$
GOF/F^2	1.005	1.030	1.024
largest diff. peak and hole (*e* A^{-3})	0.274 and −0.285	0.951 and −0.569	0.921 and −0.788

evaporation of the solvent under reduced pressure, the solid residue was washed with diethyl ether (3 × 20 mL) to remove the ferrocene and dried in vacuo. The red residue was then dissolved in a minimum amount of dichloromethane, and the solution was layered with pentane to afford red crystals of **5**. A crystal from this crop was used for an X-ray structure determination. Yield: 0.36 g (0.60 mmol, 85%). No mp detected up to 265 °C. $\mu_{eff} = 2.14\ \mu$B (CD_3COCD_3, 297 K). Anal. Calcd for $C_{26}H_{36}B_2F_6FeN_{12}P{\cdot}CH_2Cl_2$: C, 39.35; H, 4.64; N, 20.39. Found: C, 39.43; H, 4.63; N, 20.08. ^{1}H NMR (CD_3COCD_3): δ 14.7 (s, 18 H, *t*-Bu, $\omega_{1/2} = 40$ Hz), −11.1 (s, 6 H, $\omega_{1/2} = 60$ Hz, H-5), −13.8 (s, 6 H, $\omega_{1/2} = 60$ Hz, H-4), −63.4 (broad hump, H-3, $\omega_{1/2} = 500$ Hz). HR-ESI$^+$: calcd for C$^+$, 594.2721; found, 594.2733.

Bis{*tert*-butyl[tris(3-methylpyrazolyl)]borato}iron(III) Hexafluorophosphate, [Fe(*t*-BuTp^{Me})$_2$]PF$_6$ (6). A Schlenk flask was loaded with Li[*t*-BuTp^{Me}] (**1b**; 3.20 g, 10.00 mmol), $FeCl_2(THF)_{1.5}$ (1.17 g, 5.00 mmol), a magnetic stir bar, and 100 mL of dichloromethane. A purple slurry formed immediately upon stirring. The purple suspension was stirred at room temperature for 24 h. Ferrocenium hexafluorophosphate (1.59 g, 4.80 mmol) was added to the solution, and the stirring was continued for an additional 12 h. The reaction mixture was filtered, and the volume of the solvent was reduced until a minute amount of solid formed. By the slow addition of a large amount of pentane, red-orange microcrystals separated. These were filtered off and dried in vacuo. A crystal from this crop was used for an X-ray structure determination. Yield: 2.72 g (3.30 mmol, 69%). No mp detected up to 265 °C. $\mu_{eff} = 2.29\ \mu$B (CD_3COCD_3, 297 K). Anal. Calcd for $C_{32}H_{48}B_2$F6FeN12P: C, 46.69; H, 5.88; N, 20.42. Found: C, 46.62; H, 5.87; N, 21.02. ^{1}H NMR (CD_3COCD_3): δ 13.7 (s, 18 H, *t*-Bu, $\omega_{1/2} = 47$ Hz), 4.8 (s, 18 H, Me, $\omega_{1/2} = 94$ Hz), −8.1 (s, 6 H, $\omega_{1/2} = 70$ Hz, H-5), −10.1 (s, 6 H, $\omega_{1/2} = 70$ Hz, H-4). HR-ESI$^+$: calcd for C$^+$, 678.3660; found, 678.3667.

X-ray Crystal Structure Determinations. Suitable crystals of compounds **4**, **5**, and **6** for data collection were selected and mounted with epoxy cement on the tip of a glass fiber. Crystal, data collection, and refinement parameters are given in Table 1. Diffraction intensity data were collected with a Kappa-CCD Enraf-Nonius diffractometer equipped with a bidimensional CCD detector[47] employing graphite-monochromated Mo Kα radiation ($\lambda = 0.710\,73$ Å), with $2\theta_{max} = 60°$, 157 frames via 2.0° ω rotation, and 4 s per frame for **4**; $2\theta_{max} = 60°$, 652 frames via 0.8° ω rotation, and 5 s per frame for **5**; and $2\theta_{max} = 54°$, 185 frames via 1.6° ω rotation, and 20 s per frame for **6**. The cell parameters were obtained with Denzo and Scalepack[48] with 10 frames (ψ rotation: 1° per frame). Lorenz and polarization corrections were applied. The space groups were chosen on the basis of the systematic absences in the diffraction data. All three of the structures were solved using the direct methods,[49] completed by subsequent Fourier syntheses, and refined by full-matrix least-squares procedures on reflection intensities (F^2).[50] The absorption was not corrected. In compound **4**, the positions of the hydroxyl proton were determined from the electron difference map and refined. There are two chemically equivalent but crystallographically independent molecules in the asymmetric unit of **5**. In all three cases, the non-hydrogen atoms were refined with anisotropic displacement coefficients, and all hydrogen atoms, with the exception noted, were treated as idealized contributions. Atomic scattering factors were taken from the literature.[51] ORTEP views were generated with PLATON-98.[52] Compounds **4**, **5**, and **6** are CCDC reference numbers 274503, 274502, and 249549, respectively (see http://www.ccdc.cam.ac.uk).

(47) *Nonius Kappa CCD Software*; Nonius B. V.: Delft, The Netherlands, 1999.

(48) Otwinowski, Z.; Minor, W. Processing of X-ray Diffraction Data Collected In Oscillation Mode. In *Methods in Enzymology*; Carter, C. W., Sweet, R. M., Eds.; Academic Press: London, 1997; Vol. 276, Macromolecular Crystallography, Part A, p 307.

(49) Altomare, A.; Burla, M. C.; Camalli, M.; Cascarano, G. L.; Giacovazzo, C.; Guagliardi, A.; Moliterni, A. G. G.; Polidori, G.; Spagna, R. *J. Appl. Crystallogr.* **1999**, *32*, 115−119.

(50) Sheldrick, G. M. *SHELX97. Program for the Refinement of Crystal Structures*; University of Göttingen: Göttingen, Germany, 1997.

(51) *International Tables for X-ray Crystallography*; Wilson, A. J. C., Ed.; Kluwer Academic Publishers: Dordrecht, The Netherlands, 1992; Vol. C.

(52) Spek, A. L. *PLATON-98, A Multipurpose Crystallographic Tool*; Utrecht University: Utrecht, The Netherlands, 1998.

Scheme 1. General Synthetic Route to [t-BuTp^R]$^-$ Ligands

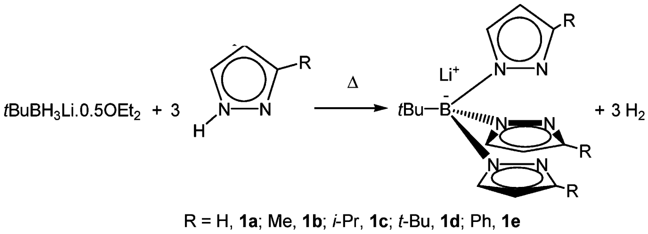

Scheme 2. Synthesis of the Thallium {*tert*-butyl[Bis(3,5-dimethylpyrazolyl)]borate} Salt **3**

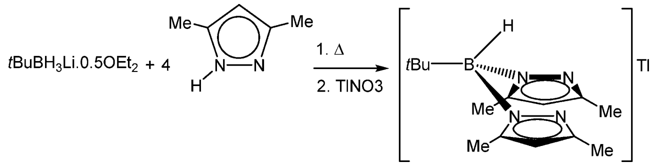

Results and Discussion

Syntheses and Spectroscopic Characterization of the *tert*-Butyl-poly[(pyrazol-1-yl)]borate Ligands. The lithium salts of the parent *tert*-butyl-tris(pyrazol-1-yl)borate, Li[t-BuTp^R] (R = H, **1a**), and of its four 3-substituted counterparts (R = Me, **1b**; i-Pr, **1c**; t-Bu, **1d**; Ph, **1e**) were readily prepared by the melt reaction of Li[t-BuBH$_3$]·0.5Et$_2$O with a slight excess (ca. 3.4 equiv) of the appropriately substituted pyrazole in yields ranging from 64 to 90% (Scheme 1). As indicated by ^{1}H NMR spectroscopy, the ligands were obtained free of contamination by the starting pyrazole after washing with hexane. However, in the cases of **1b**−**d**, vacuum distillation is first needed to remove excess Hpz^{Me}, Hpz^{i-Pr}, and Hpz^{t-Bu}, respectively. Although satisfactory elemental analyses of the lithium salts **1a**−**e** could not be obtained, possibly because of traces of starting pyrazole or partial hydrolysis (vide infra) or complete degradation (see the Supporting Information), these crude products are suitable for reaction with transition-metal salts. To overcome the problem of impure samples, we decided to prepare the corresponding thallium salts. Despite their high toxicity, Tl[Tp^R] complexes are quite common reagents for [Tp^R]$^-$ ligand transfer and ligand characterization in the case of the more sterically demanding scorpionate ligands.[2,3,53−58] Thus, the metathesis of Li[t-BuTp^R] with TlNO$_3$ yields analytically pure thallium salts Tl[t-BuTp^R] (R = H, **2a**; Me, **2b**; i-Pr, **2c**; t-Bu, **2d**; Ph, **2e**) that were further handled with the appropriate caution. Both the lithium and the thallium salts were obtained as white powders, soluble in polar organic solvents, and slightly soluble in aromatic solvents (benzene and toluene) but insoluble in aliphatic solvents.

The ^{11}B NMR spectrum of **1c** reveals one signal at δ = 3.79, thereby testifying to the presence of a tetracoordinated boron atom.[59] The room-temperature ^{1}H and ^{13}C NMR spectra of compounds **2a**−**e** in acetone-d_6 were deceptively (vide infra) simple, suggesting a C_3 symmetrical structure in solution. The spectra indicate that all three rings are equivalent, because only one signal is observed for each type of proton or carbon nucleus. This is the typical room-temperature NMR behavior for Tl[Tp^R] complexes. The exchange of Tl$^+$ for Li$^+$ has no significant effect on the ^{1}H NMR parameters of the [t-BuTp^R]$^-$ ligands under study (see the Experimental Section).

In the ^{1}H and ^{13}C{^{1}H} NMR spectra of the parent salt Tl[t-BuTp] (**2a**), the singlet resonances at δ_H = 0.92 and δ_C = 29.5 are assigned to the methyl groups of the *tert*-butyl substituent at boron. The pyrazolyl rings give rise to two doublets at δ_H = 7.60 (H-5) and 7.17 (H-3) and a doublet of doublets at δ_H = 6.24 (H-4) with corresponding ^{13}C chemical shifts δ_c = 136.5 (C-5), 139.2 (C-3), and 104.5 (C-4). These data together with the relative intensities of the four proton signals (9:6:6:6) are in accord with the proposed structure for **2a**. The ^{1}H NMR spectra of **2b**−**e** resemble those of **2a** except for the transformation of the H-4 resonance into a doublet and the replacement of the H-3 doublet by the additional signals due to the hydrocarbyl substituent protons at C-3 of the pyrazolyl ring. Interestingly, the ^{13}C chemical shifts of the methyl carbon of the t-Bu group at boron as well as the C-4 and C-5 resonances of the *tert*-butyl-tris(pyrazolyl)borate framework are almost identical for all five of the salts, **2a**−**e**, studied. In contrast, the C-3 carbon resonance is sensitive to the nature of the substituent, spanning a range of more than 20 ppm: δ_c = 139.2 (**2a**), 143.2 (**2b**), 152.2 (**2e**), 159.5 (**2c**), and 162.7 (**2d**). This gradual downfield shift of δ_{C-3} (H < Me < Ph < i-Pr < t-Bu) may express a subtle steric/electronic interplay of the hydrocarbyl groups. In all of the cases, the ^{13}C signal of the tertiary carbon atom of the *tert*-butyl boron substituent is broadened beyond detection, which has to be attributed to the quadrupolar relaxation of the adjacent boron nucleus.[59]

The reaction of 3,5-dimethylpyrazole (4 equiv) with t-BuBH$_3$Li·0.5Et$_2$O under the same conditions as those used to prepare the above-described symmetrical [t-BuTp^R]$^-$ anions afforded exclusively the *tert*-butyl-bis(3,5-dimethylpyrazolyl)borate derivative, isolated in 33% yield as its thallium salt Tl[t-BuBp^{Me2}] (**3**) after in situ metathesis with TlNO$_3$ (Scheme 2). The structure of **3** was established from an elemental analysis and spectroscopic studies. The solid-state IR spectrum shows the characteristic ν(B−H) bond stretch at 2458 cm^{-1}, and the ^{1}H NMR spectrum exhibits four sharp resonances with the relative intensities 2:6:6:9 attributed to H-4, two types of methyl, and the *tert*-butyl protons, respectively. The steric bulk of the *tert*-butyl substituent at boron blocks the substitution of the third hydride, and any increase of the temperature or of the reaction time only causes complete degradation of the intermediate lithium salt Li[t-BuBp^{Me2}]. It appears that the

(53) Dias, H. V. R. *Comprehensive Coordination Chemistry II*; Elsevier: New York, 2004; Vol. 4, pp 383−463.
(54) Janiak, C. *Coord. Chem. Rev.* **1997**, *163*, 107−216.
(55) Rheingold, A. L.; Liable-Sands, L. M.; Golen, J. A.; Yap, G. P. A.; Trofimenko, S. *Dalton Trans.* **2004**, 598−604.
(56) Rheingold, A. L.; Zakharov, L.; Trofimenko, S. *Inorg. Chem.* **2003**, *42*, 827−833.
(57) Trofimenko, S.; Rheingold, A. L.; Liable-Sands, L. M. *Inorg. Chem.* **2002**, *41*, 1889−1896.
(58) Rheingold, A. L.; Yap, G. P. A.; Zakharov, L. N.; Trofimenko, S. *Eur. J. Inorg. Chem.* **2002**, 2335−2343.
(59) Nöth, H.; Wrackmeyer, B. Nuclear Magnetic Resonance Spectroscopy of Boron Compounds. In *NMR Basic Principles and Progress*; Diehl, P., Fluck, E., Kosfeld, R., Eds.; Springer: Berlin, 1978.

fourth group at boron must be small (H or Me) in order to accommodate three 3,5-dimethylpyrazolyl residues; *tert*-butyl simply is too bulky. To date, only Tl[Tp^{Me2}][6] and Tl[MeTp^{Me2}][27] have been reported.

Solution Dynamics. In all of the ambient-temperature ^{1}H NMR spectra of **1a**−**e** and **2a**−**e**, the resonance of H-5 (i.e., the pyrazolyl proton closest to the *tert*-butyl boron substituent) always appears as somewhat broadened compared to the others. This broadening suggested some type of fluxional behavior in these molecules and prompted us to investigate more closely the solution behavior of the parent compound Li[*t*-BuTp] (**1a**) and the 3-isopropyl-substituted derivative Li[*t*-BuTp^{i-Pr}] (**1c**). Variable-temperature ^{1}H NMR spectroscopic studies were conducted in the temperature range 173−296 K. Because the two compounds exhibit qualitatively the same behavior, only the solution dynamics of **1c** are described below and shown in Figure 1.

As mentioned above, the room-temperature ^{1}H NMR spectrum (300 MHz) of Li[*t*-BuTp^{i-Pr}] (**1c**) reveals only one set of signals which is consistent with either a static symmetric C_{3v} κ^3-tridentate structure (Chart 1, **A**) or a C_{2v} symmetric bidentate κ^2-[*t*-BuTp^{i-Pr}]$^-$ structure (Chart 1, **B**) in which the noncoordinated and coordinated rings undergo rapid exchange on the NMR time scale. Upon lowering the temperature to 173 K, a broadening of the H-5 signal rapidly occurred at ca. 250 K and decoalescence was observed at ca. 213 K (Figure 1, top), giving rise to two sets of resonances in the ratio 2:1. A similar decoalescence is seen for the H-4 resonance, as well as for the isopropyl methine signal (Figure 1, bottom). This is in agreement with the presence of two magnetically equivalent pyrazolyl rings, different from the third. Strong support for the presence of only one species in solution is provided by the single resonance observed in the ^{7}Li NMR spectra over the whole temperature range. Therefore, we conclude that the apparent equivalence of all three pyrazolyl rings at ambient temperature arises from a dynamic phenomenon involving fast exchange, on the NMR time scale, between free and coordinated pyrazolyl groups, rather than from high molecular symmetry. Structure **B** in Chart 1 depicts this situation. In such a structure, also depicted as a Newman-type projection **C**, the isopropyl methyls (labeled a) on the top (noncoordinated) pyrazole will be magnetically equivalent. The two methyl groups (b and c) at one of the bottom (coordinated) pyrazol rings will be diastereotopic but will be pairwise equivalent to the methyl groups on the other bottom pyrazole ring (b to b and c to c, respectively). Consequently, the isopropyl methyl signals are expected to decoalesce into three signals with 2:2:2 relative intensities. Indeed, this is roughly what is seen at the lowest temperature available, although complete decoalescence is yet not achieved. Related dynamic behavior has been reported by the groups of Parkin[15] and Wagner[60] for sterically crowded Tl[PhTp^{t-Bu}] and Li[fluorenyl-Tp^{t-Bu}] salts, respectively. Interestingly, we also note that the *tert*-butyl substituent at boron splits into two resonances in a 2:1 ratio at low temperatures, presumably as a consequence of hindered rotation about the carbon−boron axis. We assume that the three methyl groups and the three pyrazolyl rings adopt a staggered conformation in order to minimize nonbonding interactions, as indicated in the Newman projection (Chart 1, **C**). The two magnetically equivalent methyl groups are located in the clefts between the free and the coordinated pyrazolyl arms, leaving the third one between the two coordinated pyrazolyl rings. The two sets of signals (*t*-Bu and pyrazolyl protons) coalesce upon warming to room temperature, presumably by a site exchange that involves a gearlike mechanism.

The free energy of activation $\Delta G^{\ddagger}$ for the rotation about the boron−carbon bond in Li[*t*-BuTp^{i-Pr}] (**1c**) was calculated at the coalescence temperature (eq 1)[61] and found to be 42 ± 2 kJ/mol (T_c = 213 K). A virtually identical energy barrier was calculated for the parent ligand Li[*t*-BuTp] (**1a**), $\Delta G^{\ddagger}$ = 41 ± 2 kJ/mol (T_c = 203 K), demonstrating that the relatively distant replacement of H for *i*-Pr has no significant bearing on the rotation barrier. A substantially hindered molecular motion about the carbon−boron bond was also determined for the bimetallic salt Li[FcTpMo(CO)$_3$] using variable-temperature ^{1}H NMR spectroscopy. The energy barrier of the hindered ferrocenyl rotation was calculated to be 60 ± 2 kJ/mol.[31]

$$\Delta G^{\ddagger} = RT_c\left(22.96 + \ln \frac{T_c}{\Delta\nu}\right) \quad \text{J/mol, } R = 8.31 \text{ J/K, } T_c \text{ (K), } \nu \text{ (Hz)} \qquad (1)$$

Furthermore, a closer inspection of the ^{1}H (Figure 1, 173 K) and ^{7}Li NMR spectra at the lowest available temperature shows new weak resonances with relative intensities of ca. 5 and 10% for the pyrazolyl and *t*-Bu protons, respectively, and of 3% for the lithium resonance. We tentatively attribute these signals to the “equatorial” conformer **D** in Chart 1 (the term “equatorial” denoting the position of the pyrazolyl ring with respect to the boat configuration of the six-membered chelate ring). This structure is related to the dominant “axial” structure **B** by interchange of the uncoordinated pyrazolyl and *tert*-butyl substituents, possibly by a “ring flip” of the six-membered chelate boat conformation. Precedent for this interpretation is provided by the Parkin et al.,[15] Venanzi et al.,[62] and Jones and Hessell[63] studies of stereochemical nonrigidity within Tl[PhTp^{t-Bu}], Tp$^{R,R'}$RhL$_2$ (L$_2$ = 2 CO, norbornadiene, cyclooctadiene), and Tp^{Me2}Rh(CNR)$_2$ (R = 2,6-xylyl, neopentyl), respectively. These authors demonstrated, using ^{1}H and ^{205}Tl NMR and infrared spectroscopy,[62,63] that the solutions contained three different species having (i) two types of bidentate [Tp$^{R,R'}$]$^-$ ligands, according to whether the uncoordinated pyrazolyl group was in an axial (Chart 1, **B**) or equatorial (**D**) position, and (ii) a tridentate coordination (**A**).

(60) Bieller, S.; Bolte, M.; Lerner, H.-W.; Wagner, M. *J. Organomet. Chem.* **2005**, *690*, 1935−1946.

(61) Friebolin, H. *Basic One- and Two-Dimensional NMR Spectroscopy*, 4th ed.; Wiley-VCH: New York, 2004.

(62) Bucher, U. E.; Currao, A.; Nesper, R.; Rüegger, H.; Venanzi, L. M.; Younger, E. *Inorg. Chem.* **1995**, *34*, 66−74.

(63) Jones, W. D.; Hessell, E. T. *Inorg. Chem.* **1991**, *30*, 778−783.

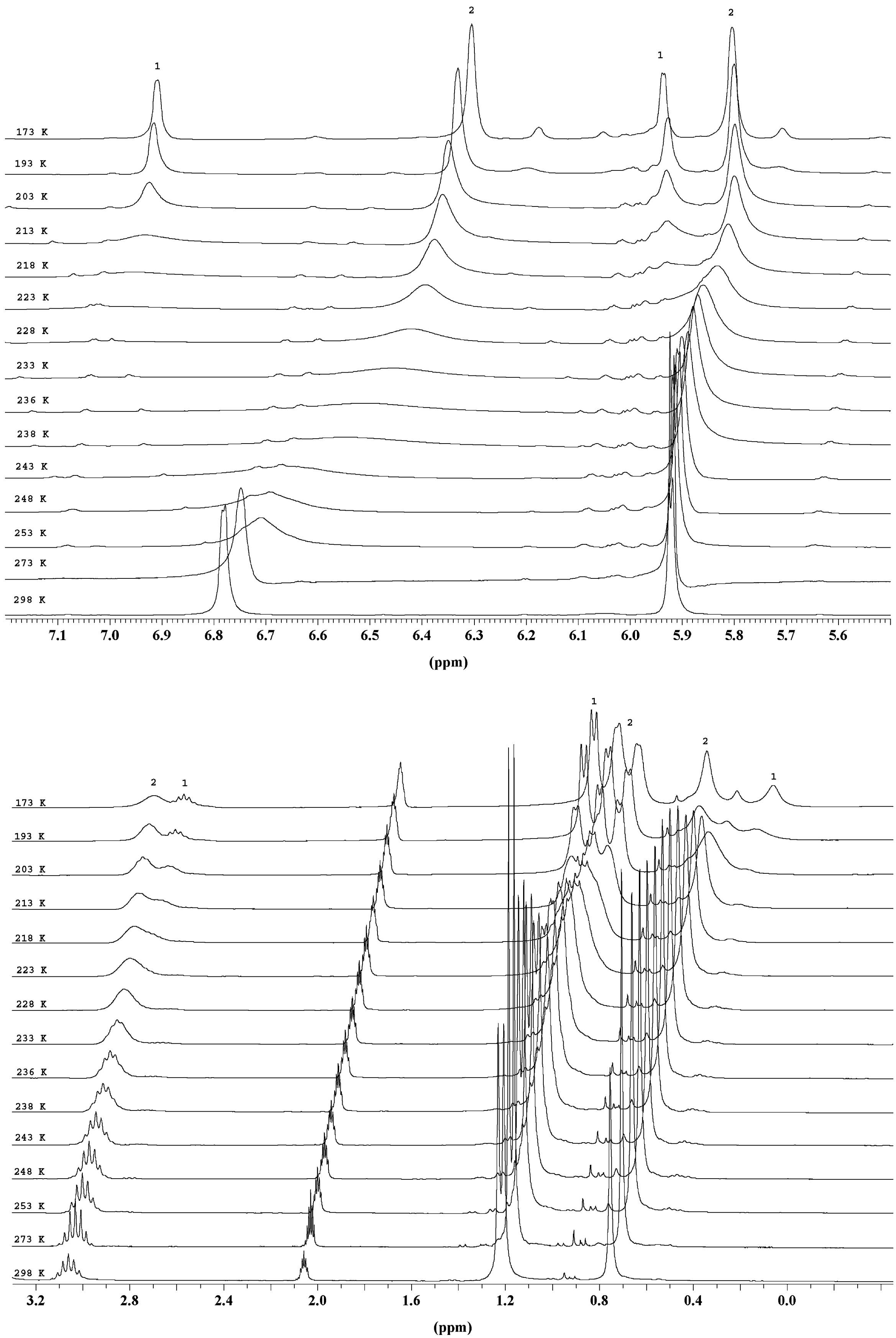

Figure 1. High-field ^{1}H NMR spectra (300 MHz) of Li[t-BuTp^{i-Pr}] (**1c**) at various temperatures in CD_3COCD_3.

Chart 1

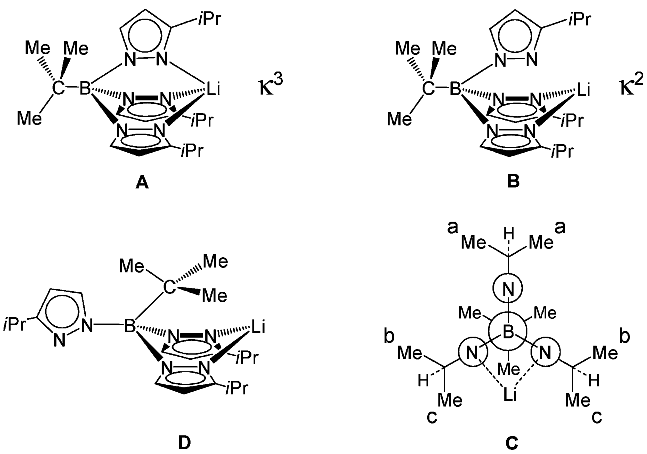

Solid-State NMR. It is of interest to know whether the structural features that were seen in solution also apply to the solid state. Therefore, Li[*t*-BuTp$^{i-\mathrm{Pr}}$] (**1c**) was subjected to a solid-state NMR spectroscopy analysis (see the Experimental Section for details). Figure 2 shows the ^{7}Li and ^{11}B MAS NMR spectra of **1c** that were reconstructed using the DM2002 program.[64] After deconvolution, both spectra clearly show two resonances (δ_{Li} = 5.35 and 4.53, δ_{B} = −0.21 and 1.21) with an integral ratio of ca. 1:4 in both cases. The data clearly indicate that the solid phase is composed of two species that can reasonably be assigned as the axial (Chart 1, **B**) and equatorial (Chart 1, **D**) isomers. The ^{13}C CPMAS NMR spectrum of **1c** is much more complicated and not readily interpretable.[65] It contains four clusters of peaks centered at δ_{C} = 26.2 (*i*-Pr and *t*-Bu), 100.9 (C-4), 136.7 (C-5), and 160.9 (C-3). Each cluster of peaks consists of a major resonance flanked by six to seven smaller resonances in a 1:4 ratio. This is in accordance with the ^{7}Li and ^{11}B NMR observations. This resonance multiplicity likely arises from a combined effect of the presence of two isomers in the solid state, diastereotopic *i*-Pr methyl groups, hindered rotations around bonds, and differences in the local environment (brought about by the three-dimensional packing of molecules) for otherwise equivalent sites.

Partial Hydrolysis of 1d: Formation and Spectroscopic Characterization of the Dimeric Heteroscorpionate Salt {Li[*t*-BuB(pz$^{t-\mathrm{Bu}}$)$_2$(μ-OH)]}$_2$ (4). Repeated attempts to crystallize the Li (**1a**−**e**) or Tl (**2a**−**e**) salts of the symmetrical tripodal ligands [*t*-BuTp$^{\mathrm{R}}$]$^-$ were unsuccessful. In contrast, colorless crystals of the dimeric salt {Li[*t*-BuB(pz$^{t-\mathrm{Bu}}$)$_2$(μ-OH)]}$_2$ (**4**), which represents a partial hydrolysis product, were isolated in about 70% yield after a solution of the sterically congested salt Li[*t*-BuTp$^{t-\mathrm{Bu}}$] (**1d**) in benzene had been exposed to the air without stirring (Scheme 3).

Crystals of compound **4** were characterized by elemental analysis and X-ray diffraction analysis (vide infra) that firmly established the dimeric nature of the complex and the cocrystallization of two molecules of 3(5)-*tert*-butylpyrazole per dimer. The ^{1}H NMR spectrum of a sample from which the free pyrazole had been removed (see the Experimental Section) exhibits only one set of resonances, two doublets at δ 7.53 (H-5) and 6.18 (H-4) and two sharp singlets at δ 1.40 (*t*-Bu-B) and 1.32 (*t*-Bu-C). The integral ratio (4:4:18:36) is consistent with the presence of four equivalent *tert*-butylpyrazolyl rings in the molecule. The OH proton was not observed. The reversal of the chemical shifts of the *t*-Bu-B and *t*-Bu-C protons with respect to those observed for the Li[*t*-BuTp$^{t-\mathrm{Bu}}$] starting material (**1d**) is noteworthy. The smooth hydrolytic reaction of one B−N bond of **1d** is reminiscent of that recently reported by Wagner and co-

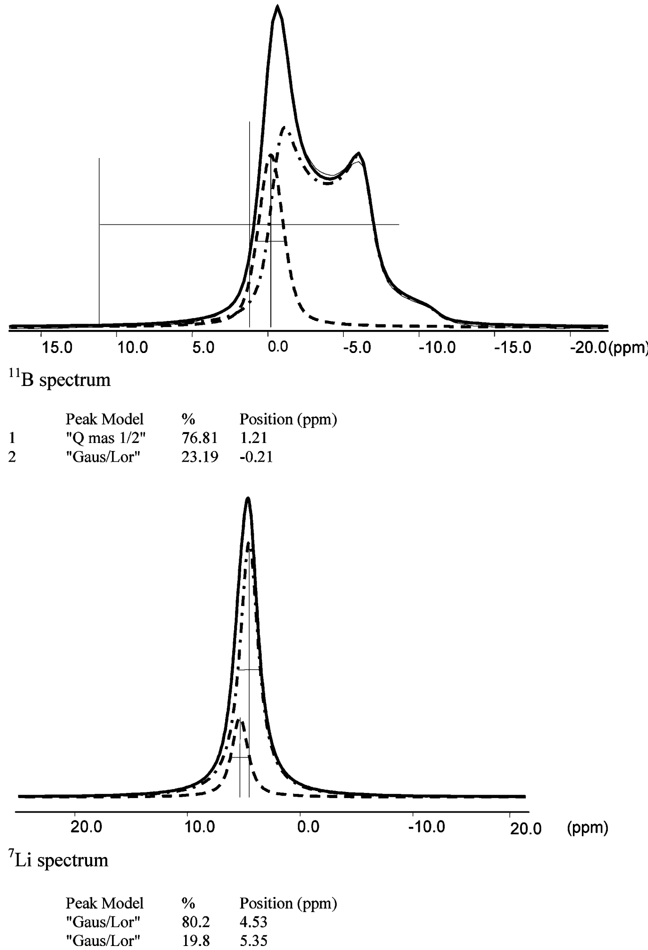

Figure 2. ^{11}B (a) and ^{7}Li (b) MAS NMR spectra of **1c**. The deconvoluted components are shown as broken lines.

Scheme 3. Generation of the Dimeric Lithium Salt **4**

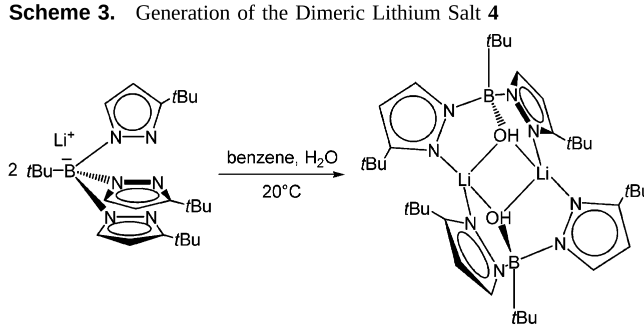

4 (70%, colorless crystals)

(64) Massiot, D.; Fayon, F.; Capron, M.; King, I.; Le Calvé, S.; Alonso, B.; Durand, J.-O.; Bujoli, B.; Gan, Z.; Hoatson, G. *Magn. Reson. Chem.* **2002**, *40*, 70−76.

(65) Claramunt, R. M.; Sanz, D.; Santa María, M. D.; Elguero, J.; Trofimenko, S. *J. Organomet. Chem.* **2004**, *689*, 463−470.

Scheme 4. Preparation of Bis{*tert*-butyl[Tris(3-R-pyrazolyl)]borato}Iron(III) Complexes

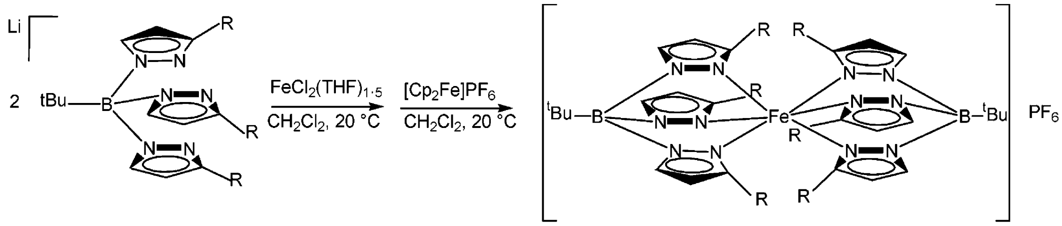

R = H, **1a**
R = Me, **1b**

R = H, **5**
R = Me, **6**

workers for the discorpionate salt $Li_2[1,3\text{-}(t\text{-}BuBpz_2)_2C_6H_4]$.[66] Left in an open vessel in THF, this compound afforded crystallographically characterized $Li_2[1,3\text{-}(t\text{-}BuB(OH)(pz))\text{-}(t\text{-}BuB(pz)_2)C_6H_4]$, which contains an unsymmetrically substituted bitopic ligand.

Synthesis and Spectroscopic Characterization of {*tert*-Butyl[tris(3-R-pyrazolyl)]borato}iron(III) Hexafluorophosphate Complexes [Fe(*t*-BuTp^R)$_2$]PF$_6$ (R = H, 5; Me, 6). The homoleptic octahedral $[Fe(t\text{-}BuTp^R)_2]^+PF_6^-$ complexes (R = H, **5**; Me, **6**) were prepared by a one-pot, two-step reaction in dichloromethane at room temperature. The first step is the metathetical reaction between 2 equiv of the lithium (**1a**−**b**) or thallium (**2a**−**b**) salts and $FeCl_2(THF)_{1.5}$ to generate neutral $Fe[t\text{-}BuTp^R]_2$ intermediates. In the second step, the Fe(II) intermediates were subjected to in situ chemical oxidation with ferrocenium hexafluorophosphate (Scheme 4). Despite the heterogeneous conditions due to the insolubility of the reagents, the PF_6^- salts **5** and **6** were isolated in 85 and 69% yields, respectively, as red microcrystalline powders. They are soluble in polar organic solvents and are air and thermally stable as solids and in solution. In contrast, the intermediate Fe(II) species suffer from extremely poor solubility in all common organic solvents, thus precluding their purification. No attempt to isolate or characterize them was done.

The identities of compounds **5** and **6** have been verified by a combination of elemental analyses, ^{1}H NMR and Mössbauer spectroscopy, and single-crystal X-ray diffraction (see below). The thermal stability of both compounds is high; their melting or decomposition points are above 265 °C (undetermined). The ESI$^+$ mass spectra of compounds **5** and **6** exhibit molecular ions (100%) corresponding to the cationic fragment with the characteristic isotopic distribution patterns (see Figures S2 and S3 of the Supporting Information).

The solution magnetic moments were determined by Evans' NMR method[40−42] (acetone-d_6, 297 K) to be 2.14 and 2.29 μB for **5** and **6**, respectively. This is in full agreement with the magnetic susceptibility measurements in the solid state [**5**, 2.35 μB (286 K); **6**, 2.34 μB (286 K) and 2.19 μB (90 K)]. These data are consistent with, but somewhat greater than, the spin-only value for a low-spin Fe(III) ion ($S = 1/2$, 1.73 μB). The deviation may be attributed to an orbital contribution rather than dominant orientational effects in the solid state.[67,68] Because the X-ray crystal structure analyses (see below) indicate that there are no obvious short contacts between the paramagnetic cations, compounds **5** and **6** do not possess linear chains necessary for cooperative magnetic properties. Analogous magnetic susceptibilities have been reported for $[Fe(Tp)_2]NO_3$, μ_{eff} = 2.61 μB in solution and 2.15 μB in the solid phase,[69] while a solid-state μ_{eff} value of 1.68 ± 0.5 μB was measured for its methylated congener $[Fe(Tp^{Me2})_2]PF_6$.[70] A room-temperature magnetic moment of 2.64 μB has been reported for a neutral, low-spin Fe(III) FeN_6 complex.[71]

The well-resolved ^{1}H NMR spectra of the paramagnetic octahedral Fe(III) complexes **5** and **6** show all six pyrazolyl moieties to be equivalent. The spectrum of **6** is consistent with unrearranged $[t\text{-}BuTp^{Me}]^-$ ligands and with all methyl substituents locating the 3 position. The peaks were sharp (except for the H-3 protons of **5**) and well-separated, and all proton signals have been assigned. The assignments were made on the basis of intensity, the effects of substitution, and line widths. Thus, the *t*-BuB (δ = 14.7 and 13.7), H-5 (δ = −11.1 and −8.1), and H-4 (δ = −13.8 and −10.1) protons of **5** and **6**, respectively, were readily identified. The H-4 and H-5 chemical shifts were assigned on the basis that those protons are progressively less upfield-shifted upon an increasing distance from the metal center.[72] These resonances, common to both complexes, appear to be characteristic of the $\{Fe[t\text{-}BuB(pz)_3]_2\}^+$ core. For the parent complex **5**, the H-3 protons resonate as a broad hump ($\omega_{1/2}$ = 500 Hz), and its high upfield chemical shift (δ = −63.4) implies close proximity to the low-spin ferric ion.[73] This would be the broadest signal if the dipolar interaction were primarily responsible for the line broadening (dipolar terms depend on the inverse of the sixth power of the distance of the proton from the electronic dipole, and so protons closest to the metal have the greatest half-widths).[74] Finally, for compound **6**, the 18 methyl protons were seen as a broad singlet ($\omega_{1/2}$ = 94 Hz) at δ 4.8, twice as intense as the *t*-Bu signal.

(66) Bieller, S.; Zhang, F.; Bolte, M.; Bats, J. W.; Lerner, H.-W.; Wagner, M. *Organometallics* **2004**, *23*, 2107−2113.
(67) Roger, C.; Hamon, P.; Toupet, L.; Rabaâ, H.; Saillard, J.-Y.; Hamon, J.-R.; Lapinte, C. *Organometallics* **1991**, *10*, 1045−1054.
(68) Paul, F.; Lapinte, C. In *Unusual Structures and Physical Properties in Organometallic Chemistry*; Gielen, M., Willem, R., Wrackmeyer, B., Eds.; Wiley: San Francisco, 2002; pp 219−295.
(69) Cho, S.-H.; Whang, D.; Kim, K. *Bull. Korean Chem. Soc.* **1991**, *12*, 107−109.
(70) Mason, S. J.; Hill, C. M.; Murphy, V. J.; O'Hare, D.; Watkin, D. J. *J. Organomet. Chem.* **1995**, *485*, 165−171.
(71) Brewer, C. T.; Brewer, G.; Shang, M.; Scheidt, W. R.; Muller, I. *Inorg. Chim. Acta* **1998**, *278*, 197−201.
(72) Jesson, J. P.; Trofimenko, S.; Eaton, D. R. *J. Am. Chem. Soc.* **1967**, *89*, 3148−3158.
(73) Armstrong, W. H.; Spool, A.; Papaefthymiou, G. C.; Frankel, R. B.; Lippard, S. J. *J. Am. Chem. Soc.* **1984**, *106*, 3653−3667.
(74) *Nuclear Magnetic Resonance of Paramagnetic Macromolecules*; La Mar, G. N., Ed.; Kluwer Academic: Dordrecht, The Netherlands, 1995.

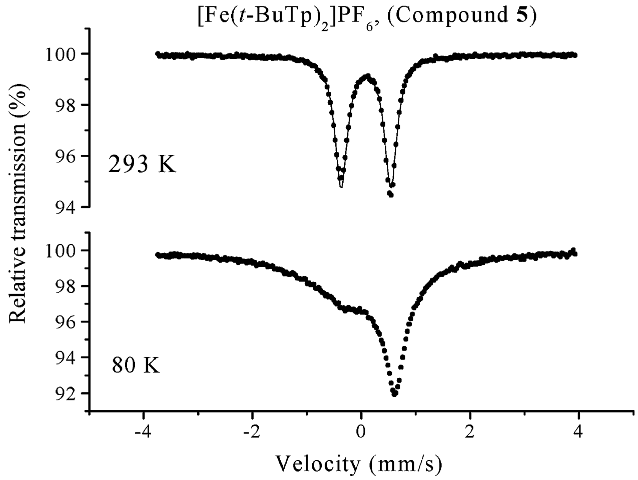

Figure 3. Mössbauer spectra of $[Fe(t\text{-}BuTp)_2]PF_6$ (**5**) and $[Fe(t\text{-}BuTp^{Me})_2]PF_6$ (**6**) obtained at 293 K (top) and 80 K (bottom). The solid lines represent fitted curves.

Table 2. Least-Squares Fitted Mössbauer Data for Compounds **5** and **6**[a]

	R=H (Compound **5**)		R=Me (Compound **6**)	
T (K)	293	80	293	80
δ (mm/s)	0.034(1)		0.086(1)	
Δ (mm/s)	0.916(1)	relaxation[b]	0.910(7)	relaxation[b]
Γ (mm/s)	0.291(1)		0.279(1)	

[a] δ: isomer shift relative to natural iron at room temperature. Δ: quadrupole splitting. Γ: full line width at half-maximum. [b] An analysis of hyperfine parameters would require more sophisticated treatment, which is beyond the scope of this work.

Mössbauer Spectral Studies. Mössbauer spectra of compounds **5** and **6** recorded at 293 and 80 K are shown in Figure 3, and the fitted Mössbauer parameters are given in Table 2. For both compounds **5** and **6**, the room-temperature spectra show a doublet with a near-zero isomer shift, δ = 0.034(1) and 0.086(1) mm/s, respectively. This, and their quadrupole splitting values of 0.916(1) and 0.910(7) mm/s, respectively, are as expected for a low-spin Fe(III) species. These Mössbauer values are significantly different in that the isomer shifts are lower and the quadrupole splittings are larger when compared to analogous low-spin Fe(II) complexes $Fe[(pzTp)_2]$ (δ = 0.40 mm/s, Δ = 0.30 mm/s) and $Fe[(Tp^{Me})_2]$ (δ = 0.45 mm/s, Δ = 0.21 mm/s at 4.2 K).[75] In fact, the room-temperature Mössbauer spectral parameters listed in Table 2 compare well with those reported in earlier studies for bis[tris(azolyl)borato]iron(III) (0.05 < δ < 0.11 mm/s, 0.77 < δ < 0.91 mm/s).[75]

At 80 K, the spectra of **5** and **6** exhibit strongly deformed line shapes (Figure 3), which occurs typically when the spin relaxation time becomes comparable either with the lifetime of the ^{57}Fe excited nuclear state or with the nuclear Larmor precession time ($1/\omega_L$). This low-temperature relaxation phenomenon is an additional evidence that in these compounds the metal ion is in the +3 oxidation state. The spectra recorded at a low temperature (80 K) exhibit a remarkable change in their quadrupole splitting values relative to the high-temperature (293 K) case. It is known that in the case of low-spin Fe(III) complexes considerable temperature dependence of the quadrupole splitting value may be observed.[76] Thus, the T_{2g}^5 (2T) state of Fe(III) corresponds to a single electron hole in an otherwise cubic triplet level. In such a case, theoretical calculations have shown that only a small distortion in the octahedral symmetry can cause this change in the quadrupole splitting value.[77] This finding is in good agreement with the X-ray data (see below). Concerning the spin state of the Fe(III) centers in **5** and **6**, the Mössbauer data alone do not allow an unambiguous determination, but the measured room-temperature effective magnetic moments (μ_{eff} = 2.35 and 2.34 μB, respectively) prove clearly that in these complexes the Fe(III) is in the low-spin ($S = {}^1/_2$) state.

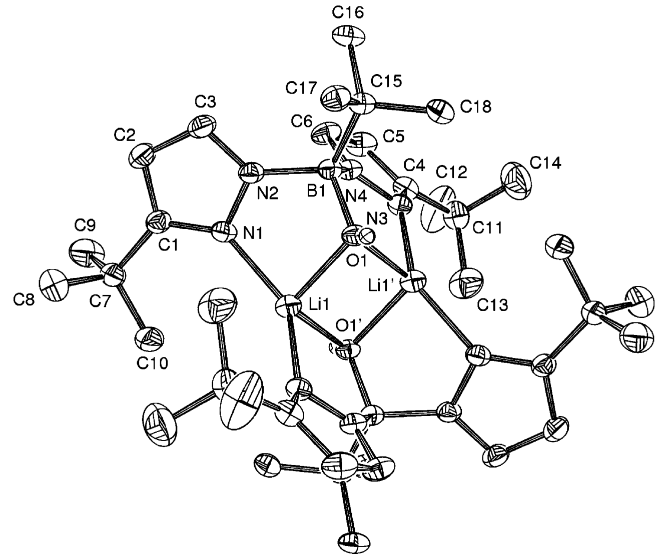

Figure 4. Molecular structure of the dimeric salt $\{Li[t\text{-}BuB(pz^{t\text{-}Bu})_2(\mu\text{-}OH)]\}_2 \cdot 2[3(5)\text{-}t\text{-}BuC_3H_3N_2]$ (**4**), showing the atom numbering scheme. Hydrogen atoms and the two free pyrazole molecules $3(5)\text{-}t\text{-}BuC_3H_3N_2$ have been omitted for clarity. Thermal ellipsoids are drawn at 50% probability.

Description of the Structure of $\{Li[t\text{-}BuB(pz^{tBu})_2(\mu\text{-}OH)]\}_2 \cdot 2(3(5)\text{-}t\text{-}BuC_3H_3N_2)$ (4). The molecular structure of this compound along with the atom-labeling scheme is presented in Figure 4. Key bond lengths and angles are listed

(75) Calogero, S.; Lobbia, G. G.; Cecchi, P.; Valle, G.; Friedl, J. *Polyhedron* **1994**, *13*, 87−97.
(76) Greenwood, N. N.; Gibb, T. C. In *Mössbauer Spectroscopy*; Chapman and Hall: London, 1971; pp 99−101.
(77) Gibb, T. C. *J. Chem. Soc. A* **1968**, 1439−1444.

Table 3. Selected Bond Lengths (Å) and Angles (deg) for Compound **4**

Bond Distances			
O(1)−Li(1)	2.016(3)	O(1)−Li(1′)	1.969(3)
O(1)−B(1)	1.4804(18)	O(1)−H(1)	0.82(2)
N(1)−Li(1)	2.016(3)	Li(1)−N(3′)	2.013(3)
Li(1)−O(1′)	1.969(3)	N(2)−B(1)	1.573(2)
N(4)−B(1)	1.581(2)	C(15)−B(1)	1.630(2)
Li(1)···Li(1′)	2.668(5)	O(1)···O(1′)	2.961(5)
Bond Angles			
N(1)−Li(1)−O(1)	86.94(11)	N(1)−Li(1)−O(1′)	129.94(14)
N(1)−Li(1)−N(3′)	139.34(15)	O(1)−Li(1)−O(1′)	95.96(12)
O(1)−Li(1)−N(3′)	108.29(13)	O(1′)−Li(1)−N(3′)	86.87(11)
B(1)−O(1)−Li(1)	109.15(11)	B(1)−O(1)−Li(1′)	115.13(11)
B(1)−O(1)−H(1)	114.4(14)	Li(1)−O(1)−Li(1′)	84.04(12)
O(1)−B(1)−N(2)	106.97(12)	O(1)−B(1)−N(4)	104.16(11)
O(1)−B(1)−C(15)	114.10(12)	N(2)−B(1)−N(4)	104.58(11)
N(2)−B(1)−C(15)	114.90(12)	N(4)−B(1)−C(15)	111.16(12)

in Table 3, and details of the data collection and refinement are provided in Table 1. The overall structure of **4** consists of centrosymmetric dimers, with normal intermolecular contacts. Compound **4** crystallizes together with 2 equiv of *tert*-butylpyrazole in the triclinic space group $P\bar{1}$ with one dimeric molecule in the unit cell. The molecule has a crystallographically imposed center of symmetry, with each heteroscorpionate ligand $[t\text{-BuB(pz}^{t-\text{Bu}})_2\text{(OH)}]^-$ presenting two terminal pyrazole residues, each bonded to a lithium center, and the crosswise bridging hydroxyl group. Because a maximum of only three Lewis basic sites can be provided by each tripodal ligand, the hydroxyl group of each heteroscorpionate fragment bridges two Li^+ cations with a Li(1)−O(1)−Li(1′) angle of 84.04(12)°. This arrangement results in tetracoordinated Li^+ ions. The structural motif exhibited by the $\{\text{Li[B(pz}^{t-\text{Bu}})_2(\mu\text{-OH)]}\}_2$ core of **4** is closely related to those observed for the $\{\text{M[B(pz}^{R2})_2(\mu\text{pz}^{R2})]\}_2$ (R = H, Me) core in the solid-state structures of the dimeric lithium salts $\{\text{Li[HB(pz}^{Me2})_2(\mu\text{-pz}^{Me2})]\}_2$[78] and $\{\text{Li[FcB(pz)}_2(\mu\text{-pz)]}\}_2$[33] and in the neutral dimeric complex $\{\text{Cu[HB(pz)}_2(\mu\text{-pz)]}\}_2$.[79] In these three cases, the two metal ions are bridged by the third pyrazolyl substituent.

The geometry about each Li^+ cation can be described as a significantly distorted tetrahedral coordination sphere, with the six bond angles (see Table 3) ranging from 86.87(11)° [O(1′)−Li(1)−N(3′)] to 139.34(11)° [N(1)−Li(1)−N(3′)]. Such strong deviations from the value of 109.28° expected for an ideal tetrahedron are also observed around the Li^+ cations in $\{\text{Li[HB(pz}^{Me2})_2(\mu\text{-pz}^{Me2})]\}_2$ [94.5(7)−139.2(10)°][78] and in $\{\text{Li[FcB(pz)}_2(\mu\text{-pz)]}\}$ [92.9(2)−144.2(2)°][33] and the Cu(I) center [93.74(9)−144.75(10)°][79] in their respective solid-state structures. The Li−N bond lengths are essentially identical [Li(1)−N(1) = 2.016(3) Å and Li(1)−N(3′) = 2.013(3) Å] and rather similar to previously reported Li−N distances involving terminal pyrazolyl groups, measured in structurally characterized four-coordinate Li^+ derivatives.[33,60,66,78,80−82]

The coordination geometry about each oxygen atom can also be regarded as a distorted tetrahedron with the four bond angles in the range 84.04(12)° [Li(1)−O(1)−Li(1′)] to 115.13(11)° [B(1)−O(1)−Li(1′)] (Table 3). The lithium and oxygen atoms form a central Li_2O_2 four-membered ring with two types of Li−O bonds, with distances of 1.969(3) and 2.013(3) Å, and O−Li−O and Li−O−Li angles of 84.40(12) and 95.96(12)°, respectively. In this inorganic parallelogram, there are no short transannular contacts between either the two lithium ions [Li(1)···Li(1′): 2.668(5) Å] or the two oxygen atoms [O(1)···O(1′): 2.961(5) Å]. The Li···Li separation is comparable to, though marginally longer than, the 2.594(7) and 2.649(8) Å and the 2.541(6) Å values found by Wagner and co-workers in the bitopic heteroscorpionate dimer $\{\text{Li}_2[1,3\text{-}(t\text{-BuB(OH)(pz))}(t\text{-BuB(pz)}_2)\text{C}_6\text{H}_4]\}_2$[66] and in Li[FcTp]_2,[33] respectively.

The bond angles at the boron center fall within the range 104.16(11)−114.10(12)° (Table 3). These distortions from an ideal tetrahedron may be a consequence of the steric demand of the *t*-Bu group and of the formation of constrained chelating BN_2LiO five-membered rings. The five-membered chelates induce constraints in the N−B−O angles [104.16(11)° and 106.97(12)°], which become substantially smaller than the idealized value 109.28°, which, consequently, opens the remaining two angles. A more regular geometry at boron is observed when chelation occurs through boat-shaped six-membered rings (BN_4Fe) as depicted below with compounds **5** and **6**. The B−O [1.4804(18) Å], B−N [1.573(2) and 1.581(2) Å], and B−C(15) [1.630(2) Å] bond lengths are quite similar to the corresponding distances in reported *tert*-butyl[bis(pyrazolyl)borate] salts.[66,82,83]

Description of the Structures of $[\text{Fe}(t\text{-BuTp})_2]\text{PF}_6$ (5) and $[\text{Fe}(t\text{-BuTp}^{Me})_2]\text{PF}_6$ (6). To definitively assign the structure of the two paramagnetic bis{*tert*-butyl[tris(pyrazolyl)]-borato}iron(III) hexafluorophosphate salts **5** and **6**, single-crystal X-ray diffraction studies were undertaken, and details of the data collection and refinement are provided in Table 1. The molecular structures of the monocationic entities of **5** and of **6** are presented in similar perspectives for the sake of comparison in Figure 5. The molecular structures of the two complexes are markedly similar, each containing an iron center sandwiched between two tridentate trinitrogen-bonding $[t\text{-BuB(pz}^R)_3]^-$ (R = H, **5**; Me, **6**) ligands, forming six-coordinated, monomeric units that are separated by normal van der Waals distances. In both cases, the tripodal ligands adopt a mutually staggered configuration. Complexes **5** and **6** crystallize in monoclinic and orthorhombic systems, $P2_1/n$ and *Pbcn* space groups, respectively, with the Fe(III) ion sitting on a center of inversion in each case. The unit cells of **5** and **6** both contain four molecules; that of the former also contains one CH_2Cl_2 solvent molecule. Moreover, complex **5** consists of two discrete centrosymmetric units, each containing an iron atom in similar octahedral sites $[\text{Fe}(t\text{-BuTp})_2]^+$, and one PF_6^- anion which occupies a general

(78) Marques, N. Personal communication.
(79) Mealli, C.; Arcus, C. S.; Wilkinson, J. L.; Marks, T. J.; Ibers, J. A. *J. Am. Chem. Soc.* **1976**, *98*, 711−718.
(80) Roitershtein, D.; Domingos, Â.; Marques, N. *Organometallics* **2004**, *23*, 3483−3487.
(81) Adhikari, D.; Zhao, G.; Basuli, F.; Tomaszewski, J.; Huffman, J. C.; Mindiola, D. J. *Inorg. Chem.* **2006**, *45*, 1604−1610.
(82) Bieller, S.; Bolte, M.; Lerner, H.-W.; Wagner, M. *Inorg. Chem.* **2005**, *44*, 9489−9496.
(83) Zhang, F.; Bolte, M.; Lerner, H.-W.; Wagner, M. *Organometallics* **2004**, *23*, 5075−5080.

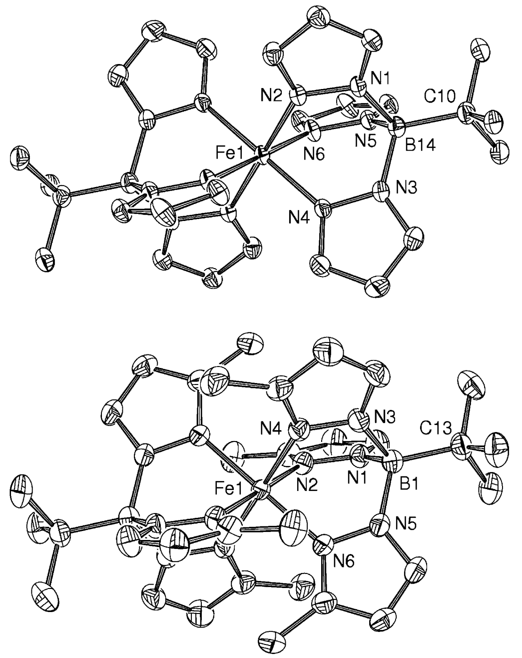

Figure 5. Molecular structures of $[Fe(t\text{-}BuTp)_2]PF_6$ (**5**, top) and $[Fe(t\text{-}BuTp^{Me})_2]PF_6$ (**6**, bottom), showing the atom numbering scheme. Hydrogen atoms and the counteranion PF_6^- have been omitted for clarity. Thermal ellipsoids are drawn at 50% probability.

Table 4. Selected Bond Lengths (Å) and Angles (deg) for Compounds **5** and **6**

	5	**6**
Bond Distances		
Fe(1)−N(2)	1.936(2)	1.951(2)
Fe(1)−N(4)	1.940(2)	1.958(2)
Fe(1)−N(6)	1.934(2)	1.956(2)
N(1)−N(2)	1.372(3)	1.369(3)
N(3)−N(4)	1.375(3)	1.373(3)
N(5)−N(6)	1.367(3)	1.372(3)
N(1)−B	1.577(4)	1.576(4)
N(3)−B(1)	1.574(4)	1.571(4)
N(5)−B(1)	1.581(4)	1.563(3)
B(1)−C′	1.627(4)	1.633(4)
Bond Angles		
N(2)−Fe(1)−N(4)	88.34(9)	89.92(9)
N(2)−Fe(1)−N(6)	87.34(9)	90.18(9)
N(4)−Fe(1)−N(6)	87.71(9)	90.10(9)
N(1)−N(2)−Fe(1)	122.31(17)	118.40(15)
N(3)−N(4)−Fe(1)	121.62(16)	118.49(16)
N(5)−N(6)−Fe(1)	122.62(16)	118.47(15)
N(2)−N(1)−B	118.5(2)	120.24(19)
N(4)−N(3)−B	119.1(2)	120.0(2)
N(6)−N(5)−B	118.4(2)	120.2(2)
N(1)−B−C′	113.9(2)	113.2(2)
N(3)−B−C′	113.4(2)	113.7(2)
N(5)−B−C′	114.9(2)	113.9(2)
N(1)−B−N(3)	104.1(2)	105.3(2)
N(1)−B−N(5)	104.8(2)	104.9(2)
N(3)−B−N(5)	104.6(2)	104.9(2)

position. The two iron sites, crystallographically inequivalent, are equivalent within the ^{57}Fe resolution (see Mössbauer spectrum, Figure 3). These two structures are similar to those observed for the other bis[poly(pyrazolyl)borato]iron(III) compounds that have been structurally characterized.[69,70,75,84−87]

Selected bond distances and angles for both complexes are presented in Table 4. The narrow range of the Fe−N bond lengths and the slight deviations of the N−Fe−N bond angles from idealized values of 90 and 180° indicate that, for both compounds, the Fe(III) center adopts an almost perfect octahedral coordination environment. Moreover, those bond parameters are in good agreement with low-spin iron(III) complexes and with the magnetic susceptibility measurements both in solution and in the solid state (see above). The Fe−N distances in high-spin Fe(III) complexes such as the half-sandwich ferrates $[Fe(Tp)X_3]^-$ (X = Cl, N_3, NCS) are considerably longer (>2.10 Å).[84−86] The six pyrazolyl rings of each complex are essentially planar, and their bond distances and angles are unexceptional (Table 4).

In the unsubstituted cationic moiety of **5**, the two crystallographically independent iron sites have bond lengths ranging from 1.934(2) to 1.940(2) Å. To the best of our knowledge, these Fe−N bond lengths are the shortest ones ever recorded for low-spin bis[poly(pyrazolyl)borato]iron(III) derivatives. They are marginally shorter than those reported for the parent cationic entities $[Fe(Tp)_2]^+$ where the Fe−N distances average 1.957 Å[86] or vary in the ranges 1.947(4)−1.960(4) Å,[69] 1.945(3)−1.975(3) Å,[85] 1.948(6)−1.964(6) Å,[75] and 1.939(5)−1.967(3) Å,[84] depending on the counteranion. This bond shortening in **5** is caused by intraligand contact between the bulky *tert*-butyl and pyrazolyl groups bonded to the boron atom,[28] as illustrated above by the variable-temperature ^1H NMR of Li[*t*-BuTp^{i-Pr}] (**1c**). The steric requirements of the *t*-Bu substituent makes the C(10)−B(14)−N angles [range: 113.4(2)−114.9(2)°] larger than the ideal tetrahedral angle (109.28°), with a concomitant decrease of the N−B(14)−N angles [range: 104.1(2)−104.8(2)°]. This intraligand contact not only induces the deviation of the ligand sphere of the boron from the ideal tetrahedral geometry but also restricts the free conformation change of the pyrazolyl rings and causes a closer approach of the N-donor atoms to the Fe center. Moreover, owing to the C_{3v} symmetrical *t*-Bu group, this intraligand contact might also be the factor that makes the six Fe−N bond lengths identical within experimental errors. The Fe−N bond distances in **5** are closer to those found in tetrakis(pyrazolyl)borato iron(III) hexafluorophosphate $[Fe(pzTp)_2]^+PF_6^-$ [range: 1.9457(17)−1.9492(16) Å].[87] In this latter case, the tripodal ligand bears also a fourth, though less bulky than the *t*-Bu group, substituent at boron.

The 3-methyl-substituted complex **6** exhibits the same structural features as its parent derivative **5**, both at the iron and at the boron atom centers. The coordination geometry around the Fe atom is almost perfectly octahedral, with short Fe−N distances ranging from 1.951(2) to 1.958(2) Å and N−Fe−N angles in the very narrow range 89.92(9)−90.18(9)° (Table 4). The Fe−N bond lengths, slightly shorter than those measured for $[Fe(Tp^{Me2})_2]PF_6$ [range: 1.960(3)−1.970(3) Å],[70] are typical distances for low-spin Fe(III) complexes. Owing to the steric demand of the *t*-Bu substituent, the

(84) Sun, Y.-J.; Yi, L.; Yang, X.; Liu, Y.; Cheng, P.; Liao, D.-Z.; Yan, S.-P.; Jiang, Z.-H. *Inorg. Chim. Acta* **2005**, *358*, 396−402.
(85) Fukui, H.; Ito, M.; Moro-oka, Y.; Kitajima, N. *Inorg. Chem.* **1990**, *29*, 2868−2870.
(86) Cho, S.-H.; Whang, D.; Han, K.-N.; Kim, K. *Inorg. Chem.* **1992**, *31*, 519−522.
(87) Trofimenko, S.; Golen, J. A.; Rheingold, A. L.; Yap, G. P. A. Personal communication.

coordination sphere at boron is also distorted with average C−B−N and N−B−N angles of 113.6(2) and 105.0(2)°, respectively. The B−C and B−N distances are virtually identical in both compounds (Table 4). The major difference between the two structures is the two N−N−Fe and N−N−B angles which vary in the opposite direction. Whereas for **6** the N−N−Fe and N−N−B angles average 118.44 and 120.15°, respectively, the corresponding angles in **5** average 122.18 and 118.7°, respectively. This expansion/contraction interplay probably serves to minimize the steric repulsions between the six methyl groups in the equatorial belt of **6**, a steric constraint that is also reflected in the B···Fe separations of 3.116 Å for **6** versus 3.083 Å for **5**.

On the basis of our structural data (Fe−N bond lengths) and data reported in the literature,[69,70,75,84−87] it appears that, for bis[tris(pyrazolyl)borato]iron(III) complexes, the substituents at C-3 of the pyrazolyl ring are not very significant in promoting the increment of the Fe−N bond length. The Fe−N distances rather are more sensitive to the apical boron substituent via the induced intraligand contact. The bulkier the boron substituent, the shorter the Fe−N bond: 1.937 Å (*t*-Bu) < 1.944 Å (pz)[87] < 1.954 Å (H)[69] (average distances for complexes unsubstituted at the pyrazolyl rings). The conclusion that the steric effect caused by the introduction of methyl groups at the 3 position of the pyrazolyl ring in Fe(III) $[Fe(RTp^{Me})_2]^+$ derivatives is not the main cause of variations of the Fe−N bond length was already drawn from an X-ray absorption spectroscopic (XANES) study.[88] At that time, no 3-methyl-substituted Fe(III) compound had been structurally characterized.[89] The spin state is the most important factor for the Fe−N bond lengthening.[84−86]

Concluding Remarks

In summary, we have prepared and characterized a series of five new *tert*-butyl[tris(3-hydrocarbylpyrazolyl)borate ligands $[t\text{-BuTp}^R]^-$ (R = H, Me, *i*-Pr, *t*-Bu, Ph), which were isolated both as their lithium and thallium salts. The parent salt Li[*t*-BuTp] and the 3-isopropyl-substituted derivative $Li[t\text{-BuTp}^{i-Pr}]$ are stereochemically nonrigid on the NMR spectroscopic time scale in solution at room temperature. The ^7Li and ^{11}B solid-state NMR spectra of $Li[t\text{-BuTp}^{i-Pr}]$ indicated that this salt exists as a mixture of axial and equatorial isomers. The latter was detected in a low-temperature (173 K) solution spectrum. The $M[t\text{-BuTp}^R]$ salts are air and thermally stable as solids but are sensitive to hydrolysis, especially those bearing the most bulky 3 substituents (*i*-Pr and *t*-Bu). The partial hydrolysis of $Li[t\text{-BuTp}^{t-Bu}]$ leads to the formation of the new heteroscorpionate Li[*t*-BuB(OH)-(3-*t*-Bupz)$_2$] that has been structurally characterized as its dimeric salt $\{Li[t\text{-BuB}(pz^{t-Bu})_2(\mu\text{-OH})]\}_2$ (**4**). The complete degradation of $Li[t\text{-BuTp}^{i-Pr}]$ afforded $Li[B(OH)_4]$, which was unambiguously identified by X-ray crystallography. Substitution of the *t*-Bu group for H at the boron center undoubtedly causes a lengthening of the B−N bond distances of this class of *tert*-butyl[tris(pyrazolyl)borate] ligands, thus rendering the B−N bond cleavage easier. The homoleptic low-spin iron(III) complexes $[Fe(t\text{-BuTp})_2]PF_6$ (**5**) and $[Fe(t\text{-BuTp}^{Me})_2]PF_6$ (**6**) have very short Fe−N bond distances. The measured Fe−N bond lengths (av. 1.937 Å) are the shortest ever reported for $[Fe(RTp^{R'})_2]^+$-type compounds. This is presumably due to intraligand repulsions resulting from the steric effect of the bulky *t*-Bu group. The intra- and interligand contacts are essential factors for producing the unique chemistry of poly(pyrazolyl)borato complexes, especially in the chemistry of Fe(II).[90] The preparation of the neutral iron(II) analogues of **5** and **6**, despite their lack of solubility, is currently being investigated in our laboratories.

Acknowledgment. Thanks are expressed to Dr. T. Roisnel (Rennes) for the determination of the crystal structure of $Li[B(OH)_4]$; to Drs. S. Sinbandhit, M. Le Floch, P. Jehan, and P. Guénot (Rennes) for helpful discussions and skillful assistance in recording variable-temperature NMR, solid state NMR, and high-resolution mass spectrometry. Financial support from the French−Norwegian AURORA program (No. 99-030); the Centre National de la Recherche Scientifique (CNRS); the Universities of Rennes 1, Toulouse III, and Oslo; and the Conseil Régional de Bretagne (grant to O.G.) are gratefully acknowledged.

Supporting Information Available: Crystallographic files in CIF format for the three reported X-ray crystal structures, the isolation and characterization of $Li[B(OH)_4]$, an ORTEP view of $Li[B(OH)_4]$, and the experimental and theoretical molecular peak isotopic distribution patterns for compounds **5** and **6** in PDF format. This material is available free of charge via the Internet at http://pubs.acs.org.

IC060458N

(88) Zamponi, S.; Gambini, G.; Conti, P.; Lobbia, G. G.; Marassi, R.; Berrettoni, M.; Cecchi, P. *Polyhedron* **1995**, *14*, 1929−1935.
(89) Allen, F. H. *Acta Crystallogr., Sect. B* **2002**, *58*, 380−388.
(90) Long, G. J.; Grandjean, F.; Reger, D. L. *Top. Curr. Chem.* **2004**, *233*, 91−122.